

UNCLASSIFIED

AD NUMBER

AD821394

LIMITATION CHANGES

TO:

Approved for public release; distribution is unlimited.

FROM:

Distribution authorized to U.S. Gov't. agencies and their contractors; Critical Technology; SEP 1967. Other requests shall be referred to Rome Air Development Center, Attn: EMCRS, Griffiss AFB, NY 13440. This document contains export-controlled technical data.

AUTHORITY

RADC per USAF ltr, 17 Sep 1971

THIS PAGE IS UNCLASSIFIED

AD821394

RADC-TR- 67-130, Volume III  
Final Report



## ANTI-JAM TECHNIQUES FOR TROPOSCATTER COMMUNICATIONS

### Volume III Tropospheric Scatter Multipath Tests

L. G. Abraham

B. B. Barrow

W. M. Cowan

R. M. Gallant

Sylvania Electronic Systems

TECHNICAL REPORT NO. RADC-TR- 67-130

September 1967

This document is subject to special export controls and each transmittal to foreign governments, foreign nationals or representatives thereto may be made only with prior approval of RADC (EMLI), GAFB, N.Y. 13440.

Rome Air Development Center  
Air Force Systems Command  
Griffiss Air Force Base, New York

When US Government drawings, specifications, or other data are used for any purpose other than a definitely related government procurement operation, the government thereby incurs no responsibility nor any obligation whatsoever; and the fact that the government may have formulated, furnished, or in any way supplied the said drawings, specifications, or other data is not to be regarded, by implication or otherwise, as in any manner licensing the holder or any other person or corporation, or conveying any rights or permission to manufacture, use, or sell any patented invention that may in any way be related thereto.

Distribution of Volumes I and II which are classified, is limited to those who have a need to know.

Do not return this copy. Retain or destroy.

ANTI-JAM TECHNIQUES FOR TROPOSCATTER COMMUNICATIONS

Volume III Tropospheric Scatter Multipath Tests

L. G. Abraham

B. B. Barrow

W. M. Cowan

R. M. Gallant

Sylvania Electronic Systems

This document is subject to special export controls and each transmittal to foreign governments, foreign nationals or representatives thereto may be made only with prior approval of RADC (EMLI), GAFB, N.Y. 13440.

AFLC, GAFB, N.Y., 16 Oct 67-98


## FOREWORD

This technical report was prepared by Sylvania Electronic Systems, Applied Research Laboratory, A Division of Sylvania Electric Products, Inc., 40 Sylvan Road, Waltham, Massachusetts, under Contract AF30(602)-3992, Project 4519, Task 451902. Authors were Leonard Abraham, Jr., Bruce B. Barrow, William M. Cowan and Robert M. Gallant. RADC Project Engineer was Walter R. Richard, EMCRS.

The experiments described in this paper involved the efforts and support of a large group. The authors wish especially to acknowledge the contributions of the following: Dr. Thomas Huang, Mr. Paul Winslow, Mr. James W. Clarke, Mr. Richard Greenspan, and Mr. Hen Su Park of the Sylvania Electronic Systems, Waltham, Massachusetts; Messrs. Frank Tomtishen and Robert Hartley, Amherst Laboratories, Sylvania Electronic Systems, Buffalo, New York; Messrs. D. Bitzer, J. N. Birch and William Waller, Department of Defense, Washington, D. C.

This technical report has been reviewed by the Foreign Disclosure Policy Office (FDPO). It is not releasable to the Clearinghouse for Federal Scientific and Technical Information because it references Volumes I and II which are classified.

This technical report has been reviewed and is approved.

Approved:   
WALTER R. RICHARD  
Project Engineer

Approved:   
RICHARD M. COSEL  
Colonel, USAF  
Chief, Communications Division

FOR THE COMMANDER:   
IRVING J. GABELMAN  
Chief, Advanced Studies Group

## ABSTRACT

The final report for this effort is prepared in three volumes. Volume III contains the results of troposcatter multipath measurements. Scattering functions are presented for data collected on other programs using a Rake receiver on two paths, one along the eastern seaboard, and the other in the Caribbean.

Volume I of the final report contains the analytical results and performance predictions for the tropo A-J systems. Volume II contains the the various A-J system descriptions.



## TABLE OF CONTENTS

<u>Section</u>		<u>Page</u>
1.0	INTRODUCTION	1
2.0	EXPERIMENTAL SYSTEM	7
	2.1 Over-land Path	7
	2.2 Over-water Path	8
	2.3 Clock Synchronization	10
3.0	CALCULATED QUANTITIES	13
	3.1 Calculation of Tap Variance	14
	3.2 Calculation of Multipath Profile Covariance Function	16
	3.3 Calculation of Scattering Function	17
	3.4 Calculation of Mean Frequency and Spectral Width	18
4.0	RESULTS	21
	4.1 Back-to-Back Test	21
	4.2 Over-land test	23
	4.3 Over-water test	43
5.0	CONCLUSIONS	51
6.0	REFERENCES	55

## LIST OF ILLUSTRATIONS

<u>Figure</u>		<u>Page</u>
1	Map of Over-land Path	3
2	Map of Over-water Path	4
3	Back-to-Back Scattering Function Record No. 117	22
4	Scattering Function Record No. 134	27
5	Scattering Function Record No. 142	28
6	Scattering Function Record No. 151	29
7	Scattering Function Record No. 163	31
8	Scattering Function Record No. 164	32
9	Scattering Function Record No. 181	34
10	Scattering Function Record No. 191	35
11	Scattering Function Record No. 201	36
12a	Scattering Function Record No. 204-1	37
12b	Scattering Function Record No. 204-3	38
13	Mean Frequency vs. Multipath Delay (Over-land Data)	40
14	RMS Spectral Width vs. Multipath Delay (Over-land Data)	41
15	Relative Auto-covariance vs. Time Shift-Record No. 3022	45
16	Scattering function, Record No. 3022	46
17	Scattering function, Record no. 3703	47
18	Mean Frequency vs. Multipath Delay (Over-water Data)	48
19	RMS Spectral Width vs. Multipath Delay (Over-water Data)	49



## SECTION 1

### INTRODUCTION

Sylvania Electronic Systems has carried on a continuing program of research in tropospheric-scatter propagation since 1964. Experiments on over-land and over-water paths have been performed. Some results were previously reported in the literature<sup>1,2,6</sup> as an application of the Rake concept to such radio paths.

The transmitted signal used in the propagation experiments was an RF carrier at about 900 MHz, phase-shift keyed by a 10-megabaud pseudo-random binary stream and subsequently filtered to a bandwidth of 10 MHz. At the receiver an identical binary stream was used in a series of 10 cross-correlators (Rake taps) where each stream was delayed 0.1 microsecond with respect to the stream in the preceding tap. A multipath resolution was obtained corresponding to a separation of the common volume into layers varying in thickness from about 200 to 550 meters depending upon the test path and the height of the layer.

During testing the multipath structure could be observed directly by looking at the magnitudes of the tap outputs, displayed on an oscilloscope. An alternative way of viewing the delay structure was provided by advancing or retarding the clock reference of the binary stream in 10-nanosecond steps. In this way any individual tap reference signal is caused to "sweep" through the full range of propagation delays, and the amplitude of the tap output, recorded during the sweep, gives a gross record of the multipath profile.

The principal goal of the propagation experiments, however, was to record the in-phase and quadrature components of each tap output, so that it would be possible to study the phase variations caused by fading, as well as the variations in amplitude. To obtain adequate

phase stability in the equipment, all heterodyning frequencies and timing sequences at each terminal were synthesized from a single stable oscillator.

Our digital tape records of the quadrature components contain the most detailed multipath data yet obtained for the tropospheric-scatter medium. Some of the available records have been analyzed with the help of a digital computer, and some new results are presented here with a brief review of previous results.

Data taken from two paths--one over-land path near the Eastern seaboard and one over-water path in the Caribbean--are presented and discussed. The over-land path was 440 km long, with the northern terminal near Washington, D.C., and the southern terminal at Ft. Bragg, North Carolina. The over-water path was located in the Caribbean between San Juan, Puerto Rico, and Grand Turk Island. This is a path length of about 614 kilometers. The actual routes are shown in Figures 1 and 2. It should be pointed out that the two areas differ markedly in climate, and therefore the experimental results can be expected to be different. The major differences observed in the experimental results are as follows.

The multipath time-delay spread for the over-water path was ordinarily less than 1 microsecond. This is considerably less than that for the shorter, over-land path where spreads of 3  $\mu$ s were common. However, much of the difference can be attributed to the difference in antenna size (8.5-meter diameter for the over-land tests, 18-meter diameter for the over-water tests).

The fading rates were markedly different, with several fades per second being typical of the over-land path, and one fade per several seconds being typical of the over-water path. Doppler shifts of 5 Hz

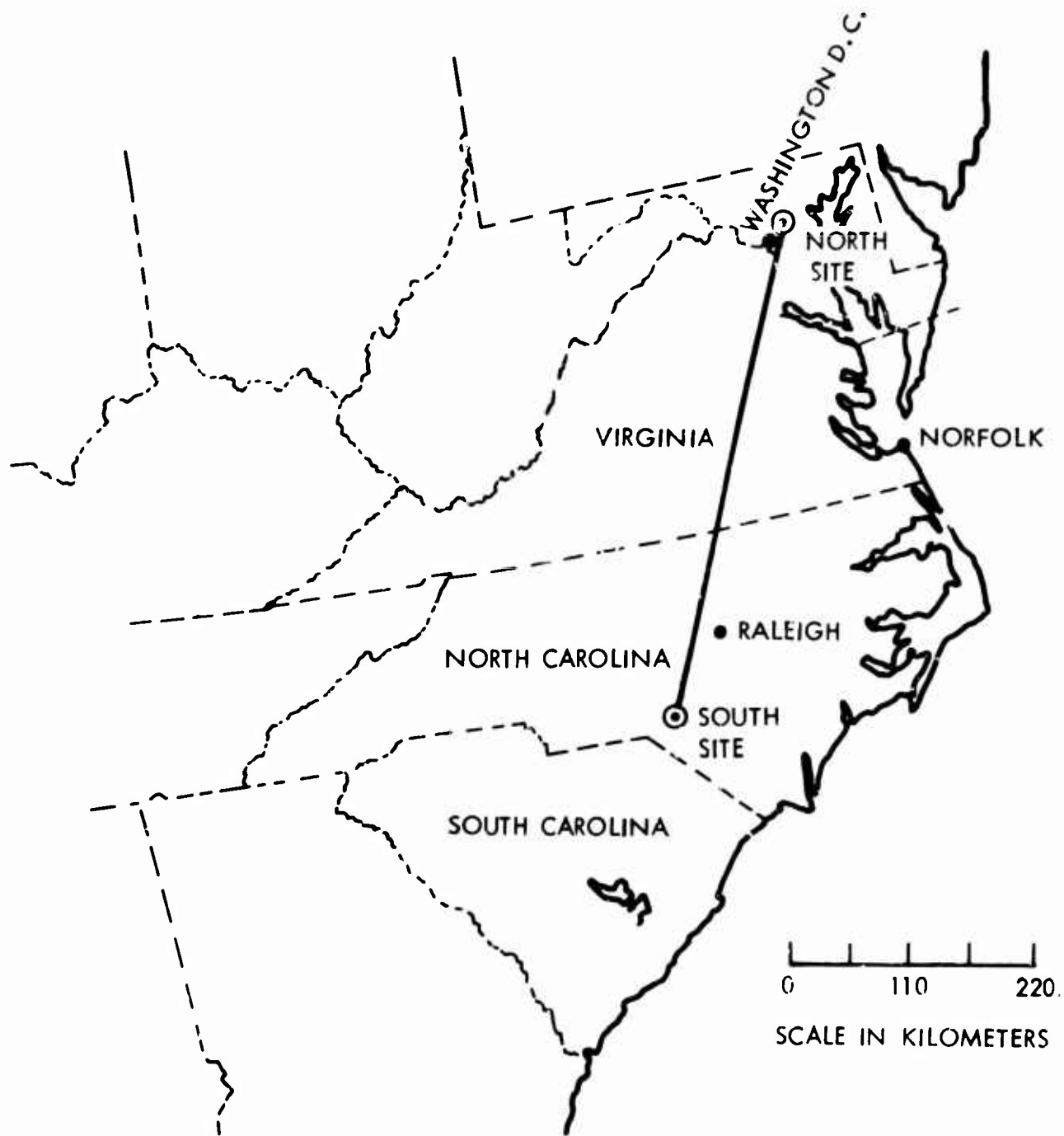


Figure 1. Map of Over-Land Path

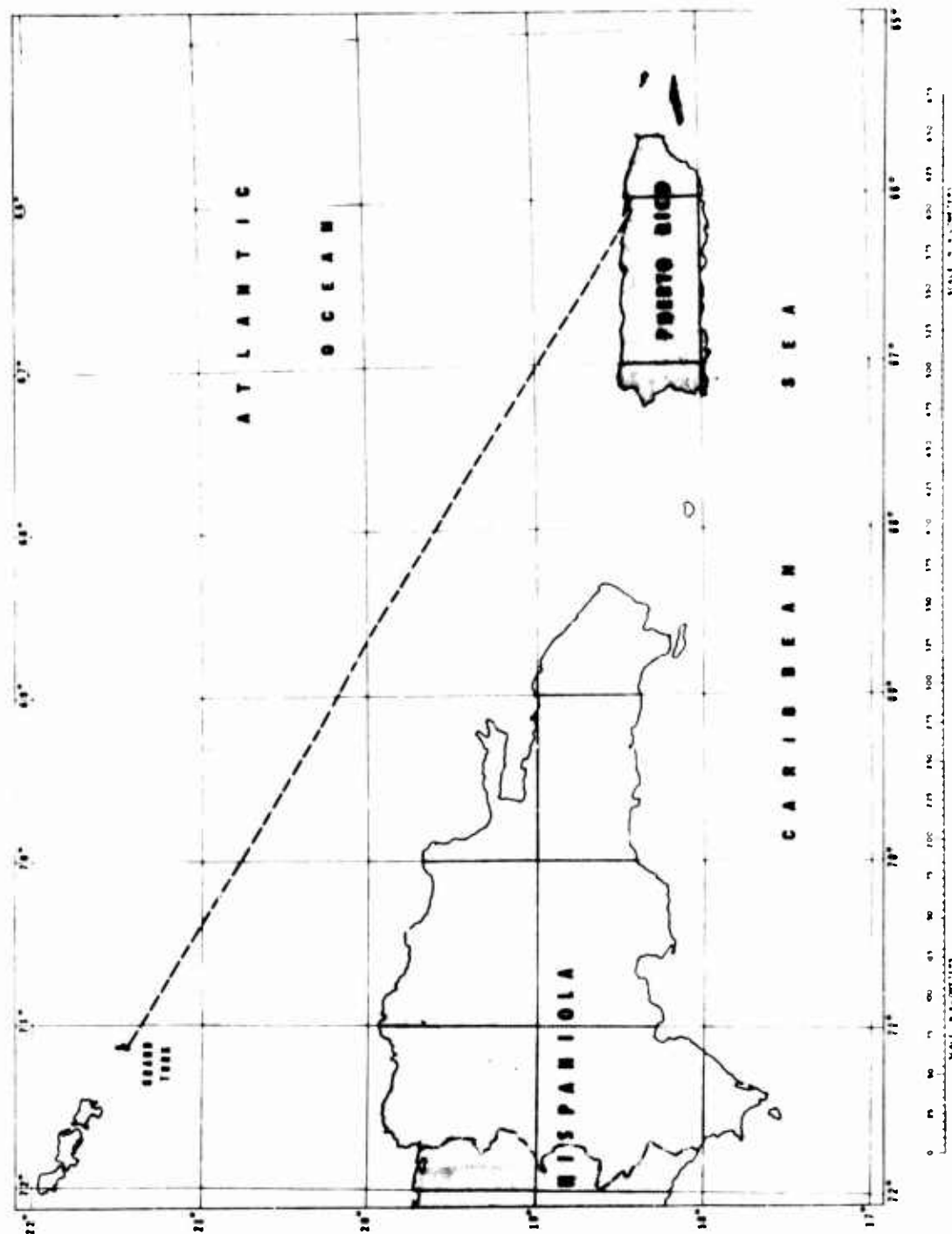


Figure 2. Over-Water Path Location

or more were sometimes observed on the over-land path, but not on the over-water path.

The following sections discuss the experimental system, the calculations, and the results obtained.

## SECTION 2

### THE EXPERIMENTAL SYSTEM

The experimental system was essentially the same for all tests and has been described in the literature.<sup>6</sup> However, there were some differences that should be pointed out. The transmitter power was 8 kW in the over-land tests and 5 kW in the over-water tests. An 8.5-meter (28-foot) parabolic dish was used at each terminal in the over-land test, while 18-meter (60-foot) antennas were used in the over-water tests.

#### 2.1 OVER-LAND PATH

Tests on the 440-km over-land path were carried out during February 1965. A standard Air Force transportable tropospheric-scatter communications equipment, the AN/MRC-98, was modified for use in these tests. The MRC-98 equipment normally operates in quadruple diversity, with two spaced antennas, differing in polarization, at each terminal. For the Rake tests, only one antenna at each terminal and one transmitter were used, with the Rake transmitter feeding the MRC-98 exciter and the Rake receiver operating from a single IF output of the MRC-98.

The transmitting site was located at the south terminal, Ft. Bragg, N. C. The antenna was vertically polarized, and the signal was transmitted at a center frequency of 910 MHz.

The receiving site was located at the north terminal, approximately 20 km northeast of Washington, D.C., a great-circle distance of 440 km (about 275 statute miles) from the transmitter. The lower edge of the 8.5-meter receiving antenna was about 3.5 meters above ground. The foreground at the receiving site was concave, with a maximum de-

pression of about 10 meters at 150 meters from the antenna. The beamwidths at this terminus were checked and determined to be  $3^{\circ} \pm 0.5^{\circ}$ .

In order to estimate the dimensions of the scattering volume,<sup>3</sup> the following path model will be examined. The antennas at both terminals are assumed pointed at an elevation equal to one half their 3-dB beamwidth. The scattering volume is then defined by the intersection of the upper and lower 3 dB points. The antenna beamwidth between 3-dB points is  $3^{\circ}$ .

Then the bottom of the scattering volume is at 3 km and the top of the scattering volume is at 14 km. The successive tap outputs of the Rake system represent contributions from layers of the common volume that are about 550 meters thick near the bottom of the common volume and 200 meters thick near the top.<sup>3</sup> The total differential time delay between the top and bottom of the scattering volume is  $4.0 \mu\text{s}$ . The path parameters are summarized in Table 1.

## 2.2 OVER-WATER PATH

As already related, this path was largely over-water, a total distance of 614 kilometers (or 382 miles). The bottom of the antenna at Grand Turk Island was about 5 meters above sea level. The antenna in Puerto Rico was located at Punta Salinas, across the bay from San Juan with the bottom of the antenna about 17 meters above sea level. For a  $4/3$  earth, this means the radio horizons were at 15 and 21 km respectively. Here, the path model for estimating the dimensions of the scattering volume is as follows. The path length of 614 km is decreased by the sum of the optical horizon distances over  $4/3$  earth. The antenna beams for this reduced path are assumed pointed at a  $0^{\circ}$  elevation. The scatter volume is defined by the intersection of the  $0^{\circ}$  elevation rays and the upper 3-dB points of the antenna beamwidth



TABLE 1  
SUMMARY OF SOME PATH PARAMETERS

	Over-land Path	Over-water Path
Operating Frequency	910 MHz	907 MHz
Path Length	440 km	614 km
Antenna Size	8.5 meters	18 meters
Beamwidth	3°	1.5°
Height of Bottom of Scattering Volume	3 km	5 km
Height of Top of Scattering Volume	14 km	9.5 km
Shell Thickness Corres- ponding to Single Tap Near Top of Common Volume	200 meters	300 meters
Shell Thickness Corres- ponding to Single Tap Near Bottom of Common Volume	550 meters	400 meters
Differential Time Delay Between Top and Bottom of Common Volume	4.0 $\mu$ sec	1.2 $\mu$ sec

( $0.75^\circ$  elevation). Although exact beam alignment data is not available for the two paths, there is good reason to believe that the antennas were aligned approximately as assumed. The bottom of the scattering volume, is then at about 5 km (16,000 feet).<sup>\*</sup> The top of the scattering volume (intersection of the upper 3 dB points of the antenna beams) would be at 10.5 km. The successive tap outputs of the lake system then represent the contributions from layers of the common-volume separated roughly by 400 meters near the bottom of the common volume and 300 meters near the top. The total differential time delay between the top and bottom of the scattering volume is  $1.2 \mu\text{s}$ . These path parameters are also summarized in Table 1.

### 2.3 CLOCK SYNCHRONIZATION

Tests were made throughout the experiments to check the stability of the frequency standards located at each end of the link. The reader will appreciate that the measurements of relative delay components depend critically on having the two clocks stay in step. These checks of relevant clock stability proceeded in two different ways. The first technique was to turn off the automatic frequency tracking system for a number of minutes and then to record the number of 10-nanosecond steps in one direction required to bring the signal back into the Rake. The second technique was to estimate the average frequency offset as shown by one pair of the quadrature components. In general, the first technique was the more useful during the over-land tests, where fading

---

<sup>\*</sup>Measurements of the refractive index<sup>7</sup> indicate that ray bending was often greater than that described by a  $4/3$  earth radius assumption. On the basis of these measurements, ray tracing results<sup>7</sup> indicate that the bottom of the common volume should have been between 4.4 and 4.8 km in December 1965, the month following our over-water tests.

was comparatively rapid, and the technique of observing quadrature components was preferred in the over-water tests, where the very slow fading made it quite effective.

We believe that during the over-water testing the frequency difference between the transmitter and receiver clocks was only a few parts in  $10^{10}$ . A difference of 1 Hz, or 11 parts in  $10^{10}$ , would have caused a drift of one tap ( $0.1 \mu s$ ) in 90 seconds. Most experiments were much longer than 90 seconds, and it was not unusual to record for five minutes without observing a drift of the multipath structure through more than a tap or two.

In the over-land experiments, we accepted data in which a drift of one tap per 100-second experiment occurred. In analyzing the data we have examined successive files and inferred the frequency offset between transmitter and receiver clocks, a technique to be discussed in greater detail. The data presented in our scattering functions have been corrected accordingly, and we believe that the Doppler frequency scales are correct to a few tenths of a hertz.

### SECTION 3

#### CALCULATED QUANTITIES

The starting point for our calculations is Eq. 2-10 of Ref. 1. This equation is reproduced below for convenience:

$$\frac{1}{2} \langle h^*(\tau; t) h(\tau + \Delta\tau; t + \Delta t) \rangle = \rho_T(\tau; \Delta t) \delta(\Delta\tau) \quad (1)$$

Here  $h(\tau; t)$  is the low-pass, complex impulse-response function of the medium,  $t$  represents time,  $\tau$  represents multipath delay,  $\rho_T$  is the multipath delay profile covariance function (sometimes called the tap-gain correlation function), and  $\delta(\Delta\tau)$  is the usual delta function. The presence of the delta function makes it clear that Eq. (1) is not an entirely proper representation of the physical situation. The difficulty is a formal one only; it comes from the fact that in setting up a mathematical model for the medium we have assumed the medium to be "frequency stationary" over all frequencies, and have imagined a probe signal which was a true impulse. In fact, the probe signal is a short pulse, and  $\delta(\Delta\tau)$  is, in the physical situation, really a narrow window function, finite and well behaved.

The actual observations, furthermore, are a series of samples of estimates of  $h(\tau; t)$ , taken for 10 different values of  $\tau$  separated by  $0.1 \mu\text{s}$ . The estimates are not perfect because short pulses, rather than impulses, are used to probe the medium, and because the observation time is finite, so that spurious noises are not entirely eliminated. In the actual experiments, each of the 20 quadrature components (the real and imaginary parts of the 10 complex-valued estimates of  $h$ ) was sampled at a rate of approximately 244 times per second, and experimental records of approximately 100 seconds in length were taken.

As has been pointed out in Ref. 1, the experiment, at best, can yield frequency resolution of no better than 0.01 Hz in the power spectrum of the fading process, and yields time resolution no better than 0.1  $\mu$ s in the multipath structure.

### 3.1 CALCULATION OF TAP VARIANCES

We may represent the output of an experiment as a set of samples  $h_{mn}$  where  $h$  is a complex number (a phasor),  $m$  is an index replacing  $\tau$ , and  $n$  is an index representing observation at time  $t$ . Thus  $m$  identifies the tap being considered in the Rake receiver, and  $n$  identifies the time of the observation.

Our first significant calculation in analyzing the data is to calculate the tap variances:

$$\overline{h_m h_m^*} = \overline{|h_m|^2} \quad (2)$$

Here the overbar indicates a sample mean taken over the  $n$  samples (i.e., a time average taken over the finite time of the experiment), and therefore the subscript  $n$  has been dropped. In performing the actual experiments, the data were recorded in five-bit digital form, with the mean of the quadrature components adjusted to fall near the middle of the quantizing range. The observed mean values were then subtracted from the samples at an appropriate point in the calculations before the variances were formed. In Eq. (2) and in the following work, we shall assume that this has been done.

If we forget about the constants that appear on both sides of Eq. (1), we may identify the expression of Eq. (2) with  $\rho_T(\tau;0)$ , where  $\tau$  is to be given a value corresponding to the particular multipath delay associated with tap  $m$  in the Rake receiver. The full set of 10 computed

values of  $\rho_T(\tau;0)$ , for each of the 10 taps, gives a multipath-power profile for the tropospheric-scatter medium. The physical significance of the multipath-power profile has already been discussed.<sup>1,2,3</sup> Roughly speaking, activity at short path delays may be associated with the lower parts of the common volume (the volume in the intersection of transmitting and receiving antenna beams), while activity at longer delays corresponds to higher altitudes.

In carrying out the calculations, the variance of  $h_m$  is of course equal to the sum of the variances of the two quadrature components. Except for experimental errors, due to noise in the system or to the small sample size, one expects the variance of the real part of  $h_m$  to be equal to that of the imaginary part.\* In this report the experiments chosen for presentation all had nearly equal quadrature variances.

Just as tap variances are calculated, it is possible to calculate cross-covariances between outputs from different taps. If the propagation mechanism which produces the signal is in fact scattering, we expect the various tap outputs to be statistically independent, except for a little correlation between signals on adjacent taps, as a result of the type of probe signal that has been used. In fact, however, finite cross-covariances have been observed. These have been checked, however, against covariances observed during back-to-back testing, and the results indicate that the observed cross-covariances may be explained entirely in terms of the equipment. This does not mean that we have demonstrated that the different tap outputs are statistically independent, but rather that the results are such that we cannot claim to have demonstrated dependence due to the propagation medium.

---

\* If these two variances were truly unequal, it would imply a phase-related type of non-stationarity in the medium.

### 3.2 CALCULATION OF MULTIPATH-PROFILE COVARIANCE FUNCTION

The multipath profile calculated from the tap variances gives us very useful information about the multipath properties of the medium, but it tells nothing whatever about the fading in time. We are thus interested in calculating the entire multipath delay profile covariance function. To carry out these calculations we follow the procedures suggested by Blackman and Tukey,<sup>4</sup> extending them to consider complex stochastic processes rather than real ones.

Our basic calculation is that of lagged products, as in the equation below

$$\overline{h_{mn}^* h_{m,n+k}} \approx \rho_T(\tau; \Delta t) \quad (3)$$

In this expression the subscript  $m$  is to be identified as before with multipath time (i.e., with a tap in the Rake),  $n$  is the subscript denoting real time, and  $k$  denotes a time shift and is to be identified with  $\Delta t$ . It may be noted parenthetically that the data were smoothed by groups<sup>4</sup> in order to reduce the amount of calculation required. This means essentially that, since the sampling rate during the experiment was much faster than the fading rate, the observations were passed through a digital low-pass filter in the computer, thus decreasing the number of calculations to be performed in order to compute each of the lagged products in Eq. (3). The averaging time used in the calculation was 100 seconds. The mean values were subtracted although this is not indicated in Eq. (3).



### 3.3 CALCULATION OF SCATTERING FUNCTION

The scattering function is obtained<sup>1</sup> by carrying out a Fourier transformation of the multipath-profile covariance function. (That is, the power spectrum of each tap output is calculated.) In carrying out this transformation, a spectral smoothing process such as "hanning," described by Blackman and Tukey,<sup>4</sup> is absolutely essential. This is because the autocovariance function, calculated as already discussed, has to be truncated where there is still significant correlation. With records of 100 seconds it is not reasonable to introduce time shifts greater than approximately 10 seconds when calculating lagged products. For the Caribbean tests it turned out that the fading was so slow that the autocovariance at shifts of 10 seconds was ordinarily still quite significant. If hanning is not performed, therefore, any sharp peak in the true power density spectrum will show up as multiple peaks in the calculated spectrum, these peaks being roughly of the  $(\sin x)/x$  type. Because of clock instability, it is difficult to analyze records that are much longer than 100 seconds. The effects of clock instability have been discussed in Ref. 1. The general effect is to cause some broadening of peaks in the spectral estimate of narrow spectra. The composite result of instability and of finite record length is such as to give a real resolution in frequency spectrum of something greater than 0.1 Hz.

It should be observed that the covariance function of Eq. (3) is real only if the power spectrum of the fading is even. In general this is not to be expected, since any frequency offset, to say nothing of any process which would make for an asymmetrical power spectrum, will introduce an imaginary part into the covariance function.

Although it is possible to plot the real and imaginary parts of the covariance function, it is difficult to interpret the results, and

for this reason the covariance function which is presented in this report is given as an envelope function only. The scattering function (tap power spectrum) is used to present the same information in what is believed to be a more easily viewed form.

### 3.4 CALCULATION OF MEAN FREQUENCY AND SPECTRAL WIDTH

The mean frequency is calculated from the discrete analog of

$$\bar{\nu}(\tau) = \frac{\int \nu V(\tau; \nu) d\nu}{\rho_T(\tau; 0)}$$

where  $V(\tau; \nu)$  is the scattering function and  $\rho_T(\tau; 0)$  is the autocovariance for zero time shift, each available for discrete values of the multipath delay time  $\tau$ . The covariance is given by

$$\rho_T(\tau; 0) = \int V(\tau; \nu) d\nu$$

The Doppler spread or spectral width is calculated from the discrete analog of

$$\sigma = \left( \frac{\int (\nu - \bar{\nu})^2 V(\tau; \nu) d\nu}{\rho_T(\tau; 0)} \right)^{1/2}$$

The mean frequency  $\bar{\nu}$  is the first moment of the power spectrum, and is a measure of the central frequency; the RMS spectral width  $\sigma$  is the square root of the second central moment of the spectrum. The former corresponds to Doppler shift in the medium or to frequency er-

rors between the transmitter and receiver clocks, which would affect each tap in an identical fashion, and the latter to Doppler spread, which is directly related to fading rate.

## SECTION 4

### RESULTS

#### 4.1 BACK-TO-BACK TESTS

Before the experiments began, the transmitter and receiver were connected back-to-back at radio frequency to assure proper operation of the equipment. Figure 3 presents a scattering function calculated from one of the back-to-back tests, Record No. 117. The spectra as plotted are normalized to the largest spectral peak, in this case at  $0.7 \mu s$  multipath delay. The tap numbers are indicated and circled adjacent to the spectra. Establishing the origin of the multipath delay time is arbitrary since the absolute path delay can not be established in the propagation tests.

In Figure 3 it is clear that the transmitter and receiver frequencies differed by 0.2 Hz, mean value, with the reference signal at the receiver being the higher. This is a fractional relative offset of  $-2.2 \times 10^{-10}$ . The negative sign indicates that the measured spectral center of the received signal is low with respect to the receiver reference frequency. Table 2 summarizes the calculation of mean frequency and spectral width for taps 2 through 4.

The scattering functions which are presented later must be interpreted in terms of the finite frequency resolution of about 0.1 Hz and the finite multipath delay resolution of about  $0.1 \mu s$ . The multipath width is a result of signal design and tap crosstalk. The relatively low tap-to-tap crosstalk level indicated in Figure 3 applies during the period in which the over-land test series was taken in February 1965. Crosstalk was slightly worse during the over-water series in November and December 1965 due to equipment readjustment.

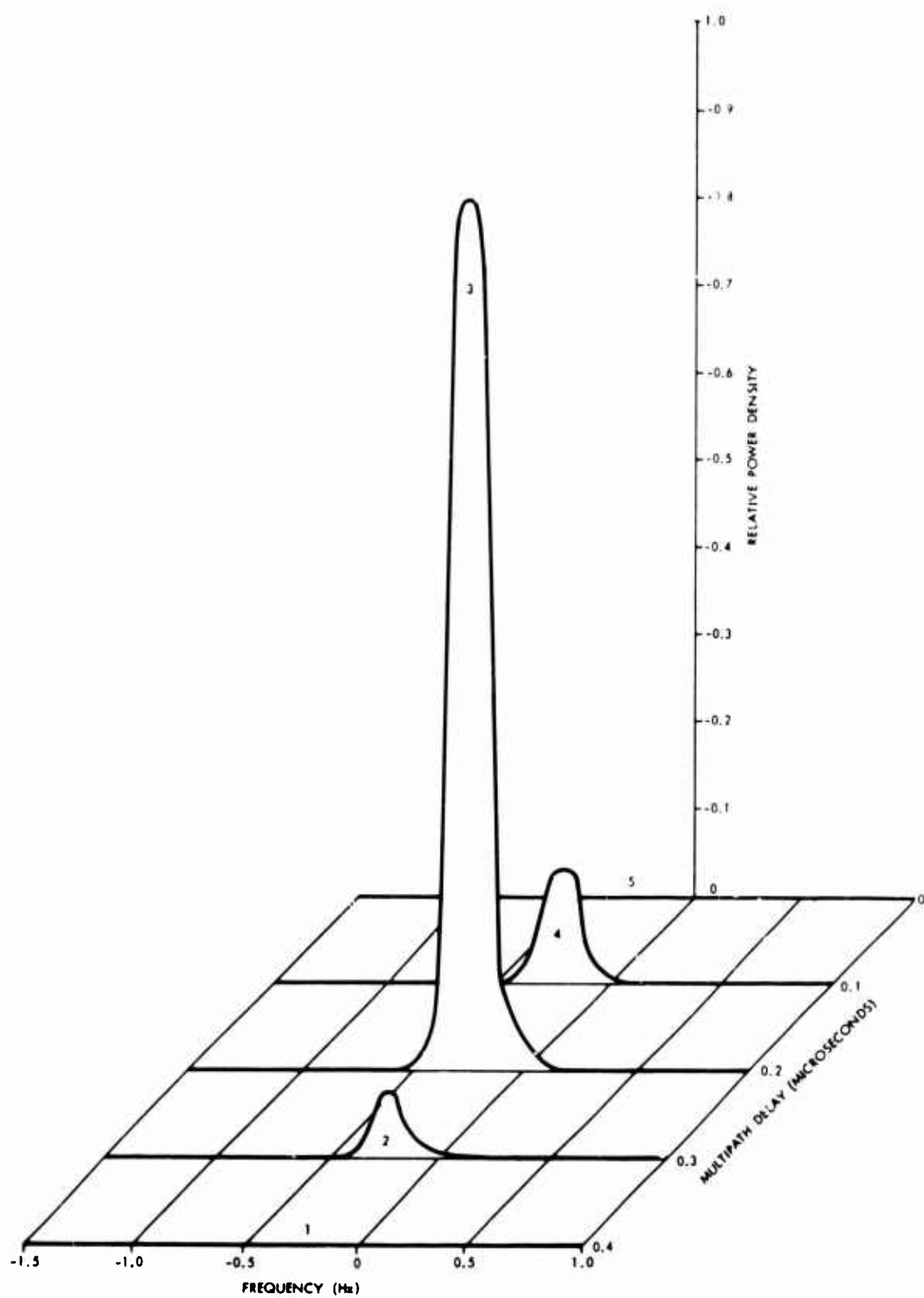


Figure 3. Scattering Function, Record No. 117, Taken During RF Back-to-Back Tests in February 1965

TABLE 2

MEAN FREQUENCY AND SPECTRAL WIDTH FOR THE BACK-TO-BACK TEST,  
RECORD NO. 117

<u>Tap No.</u>	<u>Mean Frequency (Hz)</u>	<u>RMS Spectral Width (Hz)</u>
2	- 0.25	0.13
3	- 0.28	0.11
4	- 0.22	0.10

#### 4.2 OVER-LAND TESTS

The test series conducted in February 1965 involved the 440 km path previously discussed. Scattering functions from these data are presented in Figures 4 through 12. The mean frequency and spectral widths for these scattering functions are presented in Figures 13 and 14.

Table 3 summarizes information about the records reduced for presentation here. The first two columns give the date and time (EST = GMT-5) of the recording. The column headed "Run" gives the serial number used to identify the recording throughout this report. Most records were long enough to provide several "files", each approximately 100 seconds long, for analysis, and the fourth column lists the files used for the data presented herein. The tests were made with the automatic gain control disabled, and with an adjustable attenuator set to provide appropriate levels. The setting of the attenuator is recorded to give a rough idea of relative signal strengths observed during the experiments.\* Finally, the last column lists a few pertinent comments made in the log during the experiments.

---

\*The scattering functions shown later in this report were all normalized in amplitude and therefore do not contain any information about total signal level.

TABLE 3  
MAGNETIC TAPE RECORDS FROM THE OVER-LAND TESTS ANALYZED IN THIS REPORT

Date	Starting Time (EST)	Run	File	Attenuator Setting (dB)	Operator Comments
Feb. 16	1726:20	134A	3	20	Good clock stability
16	1729:10	134B	1	20	
17	1157:20	142A	3	30	Good clock stability--longer delay taps seem to oscillate faster
17	1200:10	142B	1	30	
18	0321:10	151B	1	24	
18	0327:20	151C	1	24	
18	0333:30	151D	1	24	
18	0732:40	163	3	49	Strong duct
18	1002:57	164A	2	14	
18	1008:17	164B	1	14	
19	1331:00	181A	1	20	Good clock stability
19	1337:10	181B	1	20	
19	1343:20	181C	1	20	
19	1350:00	181D	1	20	
20	1029:00	191	1	25	Lower taps fading slowly, upper taps faster
22	1752:00	201	1	12	
23	1150:05	204	1	25	Airplane in Tap 7
23	1153:25	204	3	25	



Most of the scattering functions are constructed from multiple records. That is, a six-minute record of data was recorded; the timing at the receiver was retarded, usually by about  $0.6 \mu s$ , and a second six-minute record was recorded. In some cases, there were additional retards and recordings. Two or three 100-second files were made from each six-minute record. In analyzing the data, successive files from the same record were examined and compared. In some cases, it was observed that a second file could be made to match a first file only if the second file was shifted forward or backward by one Rake tap. In some cases a shift of one tap occurred between the first and third file. From the shift in tap delay and the interval between files a fractional frequency offset between the transmitter and receiver clocks can be inferred. In fitting together the multiple records in order to form a single scattering function, the inferred clock offsets were used to correct the Doppler frequency scale and the record-to-record timing.

It was also necessary to infer relative tap amplifications. That is, the voltage amplification was not the same for all Rake taps. We have inferred tap-amplification corrections from a comparison of successive files throughout the experiment and have applied these to the scattering functions presented here.

For the overwater tests, reported in a later section of this report, a calibration run was made, which was used to correct for unequal tap amplifications, before that phase of the experiments. The experimental adjustment of the receiver clock during this test series could be more accurately performed due to the slow fading. Therefore, no adjustment of the Doppler frequency scale of the scattering functions from the overwater test series was found to be necessary.

#### 4.2.1 Record No. 134

Figure 4 gives the scattering function for Record No. 134 taken at 1726 EST on 16 February 1965. As presented, the figure represents the composite of two separate runs. Record No. 134A was first recorded. The timing at the receiver was then retarded and Record No. 134B was started approximately 170 seconds following the beginning of 134A, file 3. Each run analyzed represents 100 seconds of data. The calculated mean frequencies and spectral widths are given in Figures 13 and 14.

A striking feature of Record No. 134 is the obvious decrease of mean frequency with increasing multipath delay. More will be said on this in the later discussion of Figure 14.

#### 4.2.2 Record No. 142

Figure 5 presents the scattering function for Record No. 142 taken at 1157 EST on 17 February 1965. This scattering function represents the composite of two records spaced by 170 seconds in starting time. In Figure 5, as in Figure 4, the decrease in mean frequency with increasing multipath delay is obvious.

#### 4.2.3 Record No. 151

Figure 6 presents the scattering function calculated from Record No. 151, recorded at 0321 EST on 18 February 1965. This figure represents the composite of three records. Record No. 151B was recorded, the receiver timing was retarded and Record No. 151C was recorded beginning six minutes after 151B. The receiver timing was again retarded and Record No. 151D was recorded beginning six minutes after 151C. The same decrease in mean frequency with multipath delay appears here as in the previous scattering functions.

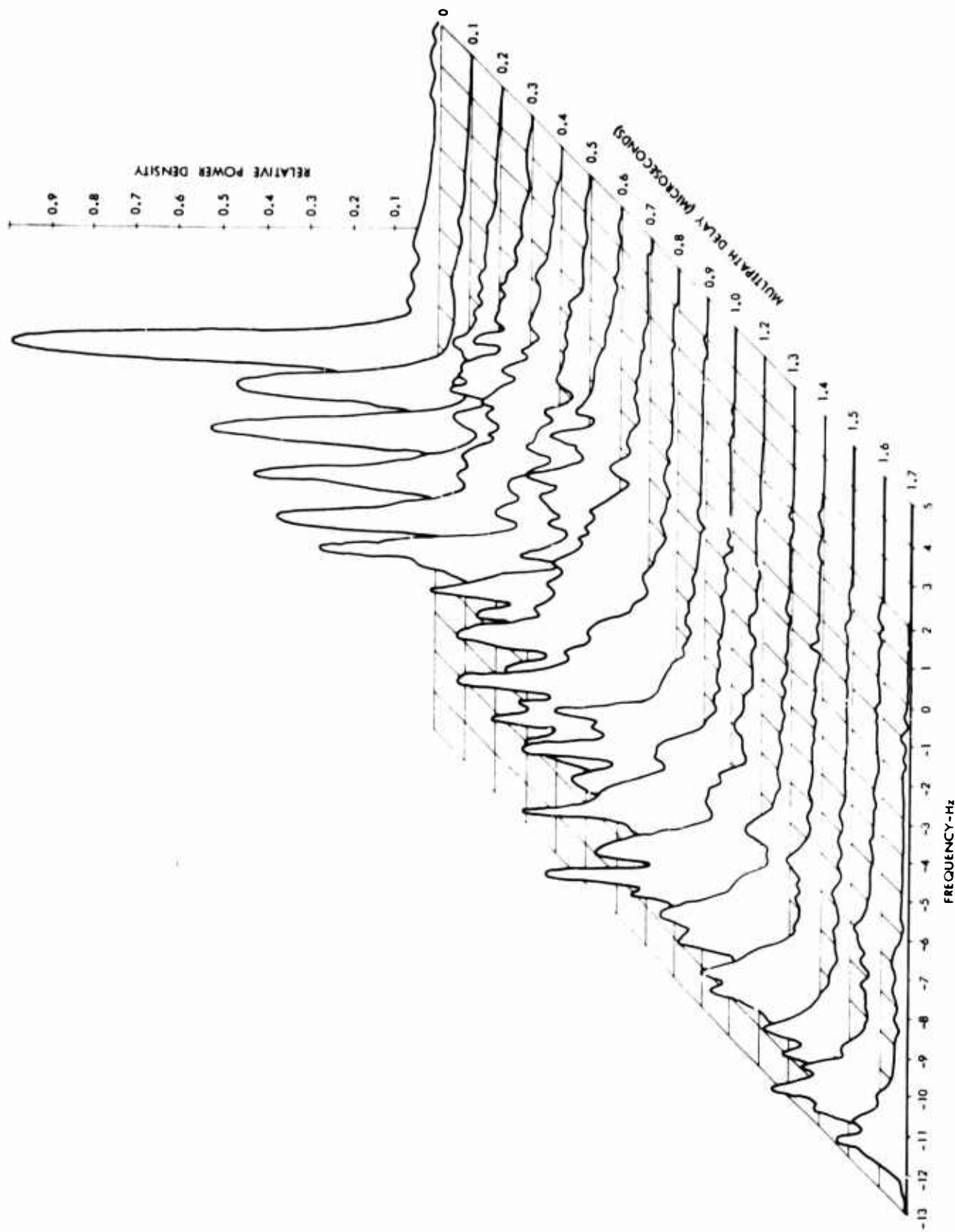


Figure 4. Scattering Function, Record No. 134

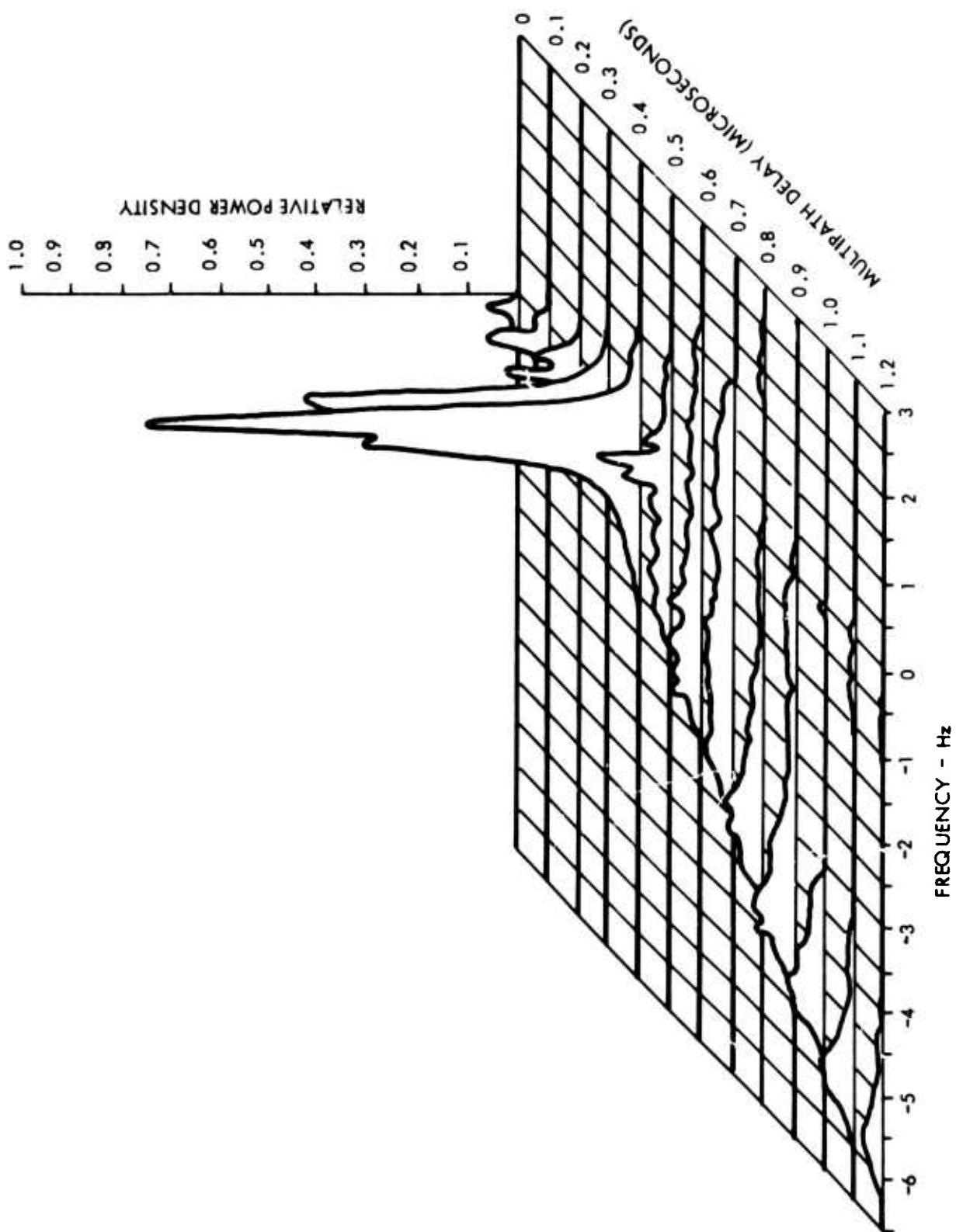


Figure 5. Scattering Function, Record No. 142

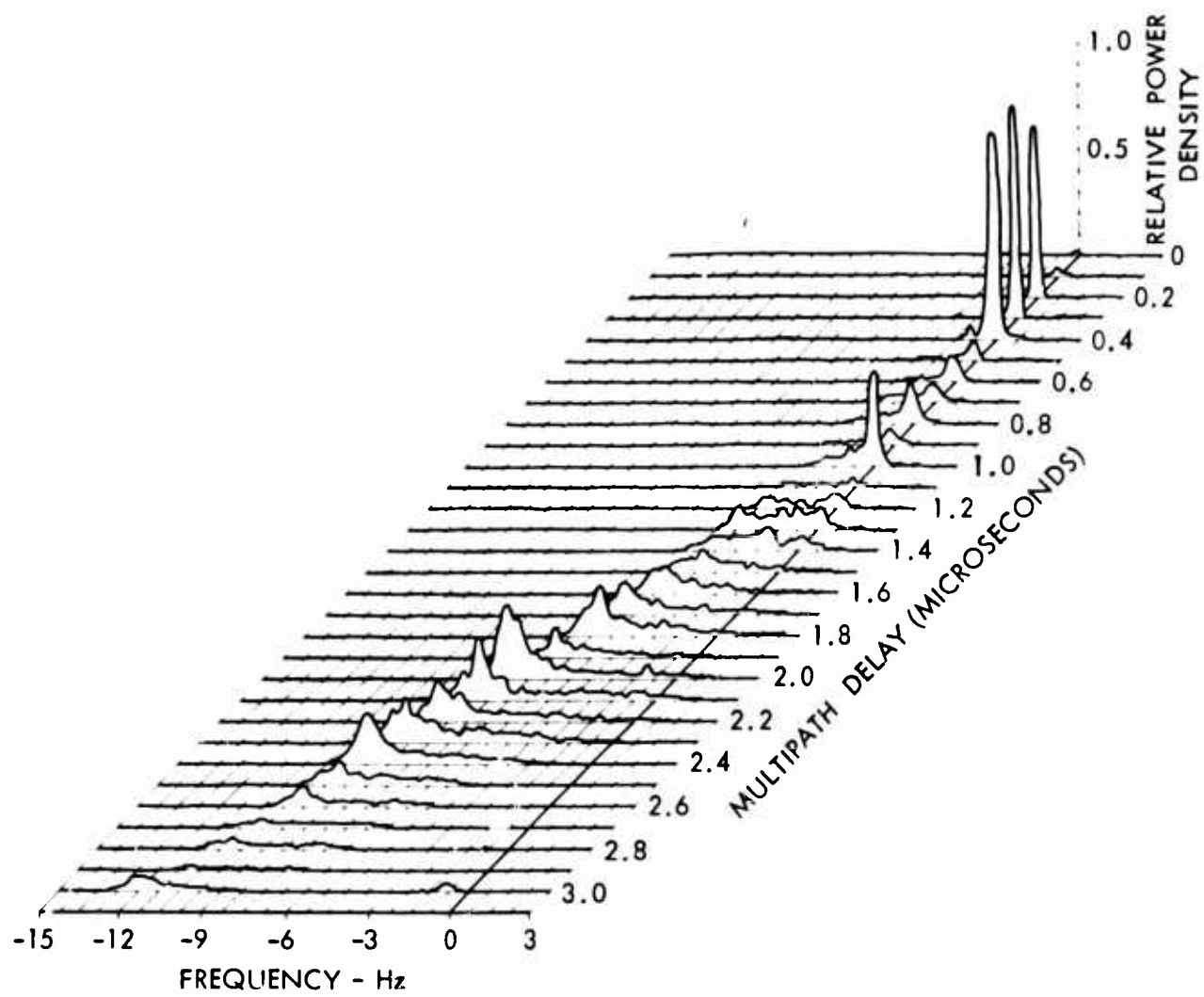


Figure 6. Scattering Function, Record No. 151

#### 4.2.4 Record No. 163

Figure 7 presents the scattering function from Record No. 163, file 3, taken at 0733 on 18 February 1965. The operator's comments indicate that a strong duct phenomenon appeared at this early morning hour. (Notice the attenuator setting in Table 3.) The spectral width for this scattering function is as narrow as that observed in the back-to-back tests, and the multipath width is only slightly wider than for the back-to-back test.

#### 4.2.5 Record No. 164

Figure 8 presents the scattering function from Record No. 164 taken at 1003 EST on 18 February 1965. This scattering function represents the composite of two runs.

Record No. 151 and 163 preceding plus this record present a brief glimpse into the history of the growth and decay of the duct in the morning of 18 February. The scattering functions from Records 151 and 164 appear quite similar. Initial delay components are centered near zero frequency and are relatively narrow (slowly fading). Successively later delay components are shifted toward more negative Doppler frequencies and are wider (relatively faster fading). The duct scattering function, and also the initial delay components for the other two scattering functions, appear relatively narrow and centered near zero Doppler frequency. It may be that the initial delay components for 151 and 164 are caused by the same scattering phenomenon which produced what we call the duct, Record No. 163, except that the level is lower. (Note the relative attenuator settings in Table 3.)

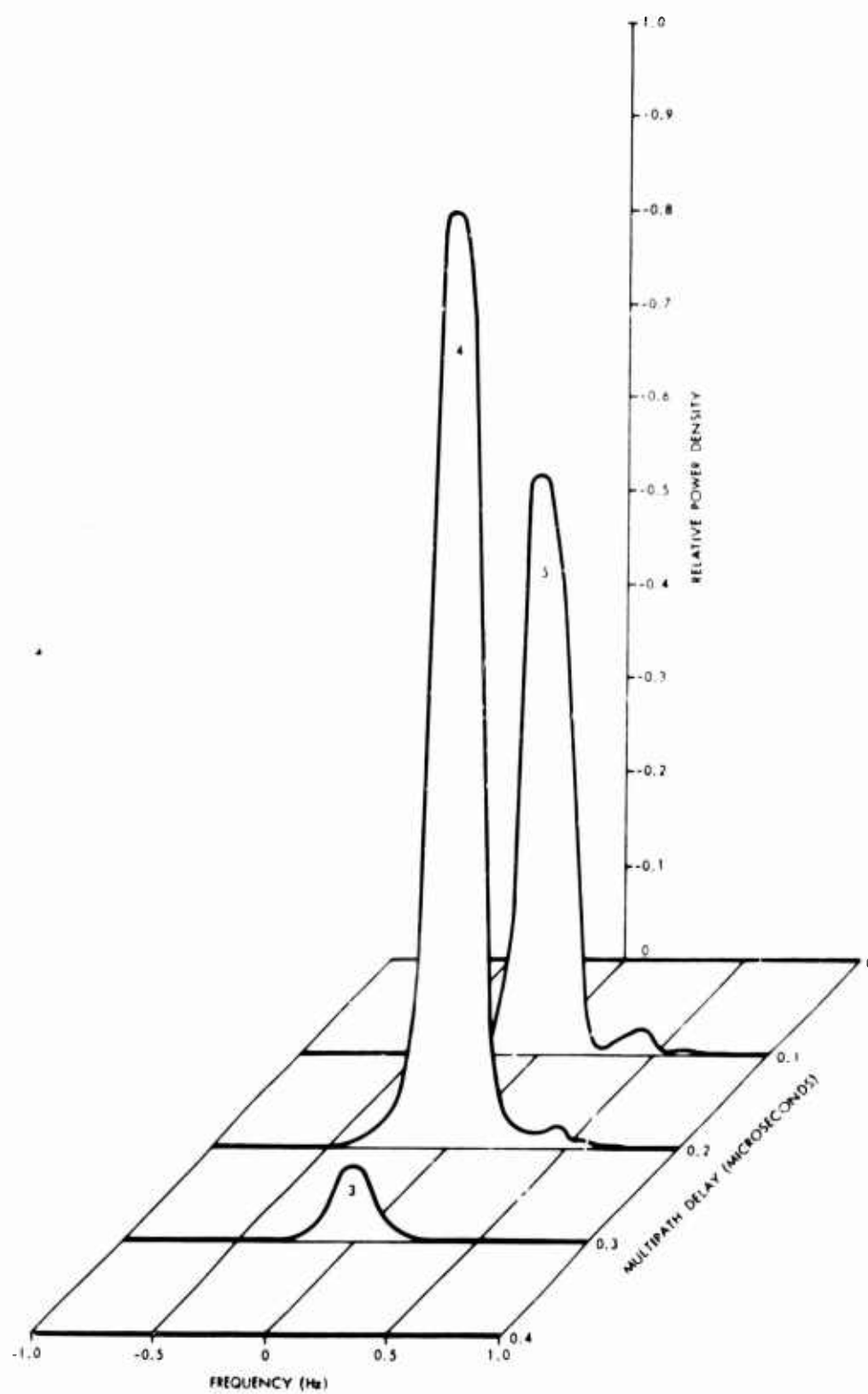


Figure 7. Scattering Function, Record No. 163



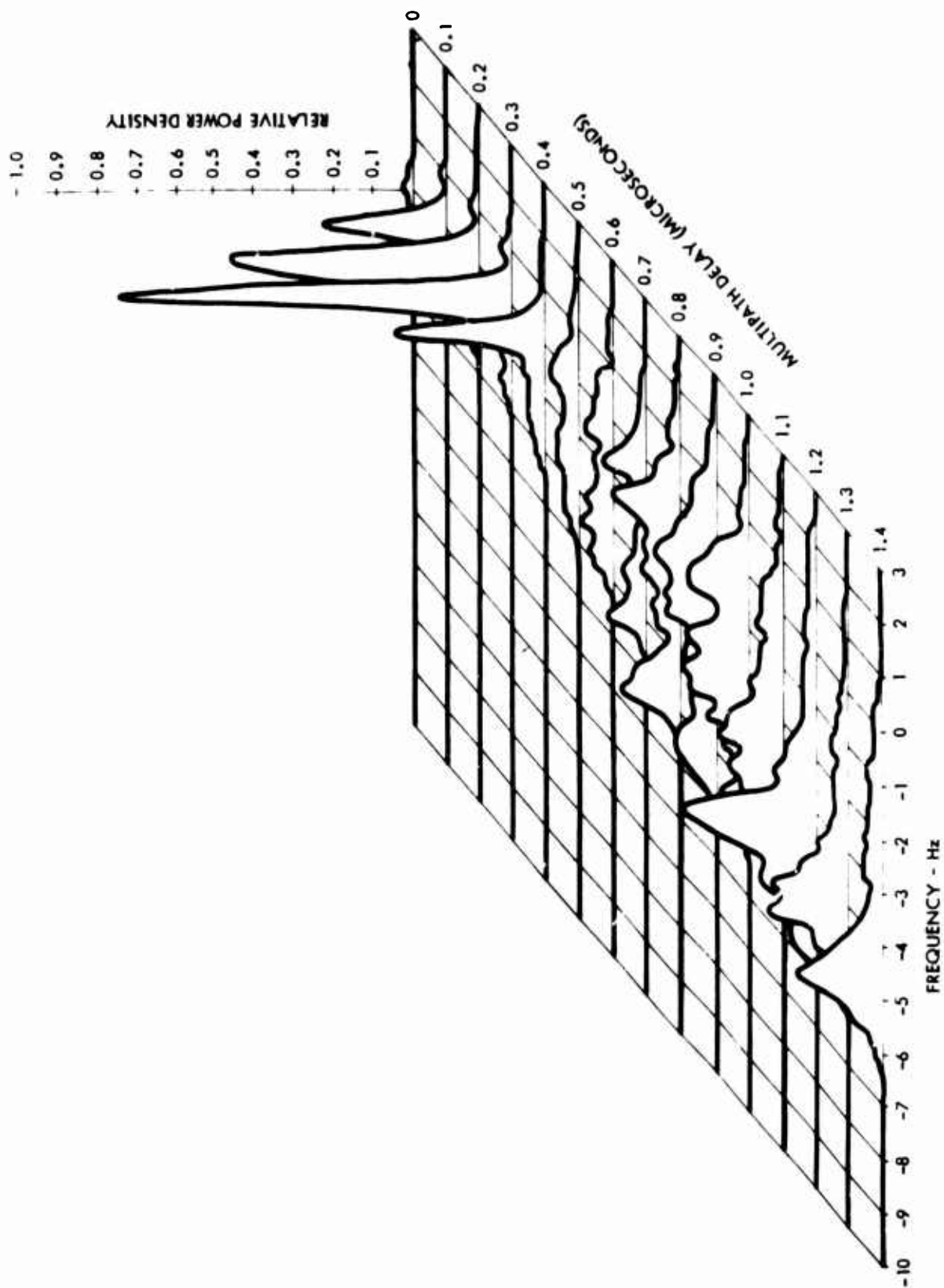


Figure 8. Scattering Function, Record No. 164

#### 4.2.6 Record No. 181

Figure 9 gives the scattering function for Record No. 181 collected at 1337 EST on 19 February 1965. This is a composite of four records. The spectral widths observed on this record are the widest of the calculated set. The mean frequencies for the individual spectra are the most negative of the calculated scattering functions. Note the three-humped spectra at delays of 1.0 to 1.4  $\mu$ s.

#### 4.2.7 Record No. 191

Figure 10 gives the scattering function for Record No. 191 collected at 1029 on 20 February 1965. The numbers written on the individual spectra are tap numbers. The operator's log makes the comment that the early taps appeared to fade more slowly than the later taps. However, the calculated spectral widths are not significantly different between the early and late taps. The mean frequency variation with delay would give rise to the noted operator's comment based on observation of the quadrature components. A mean frequency difference would give the appearance of rapid fading in the quadrature components, whereas the envelope of the tap output would fade more slowly.

#### 4.2.8 Record No. 201

Figure 11 gives the scattering function calculated from Record No. 201. The tap numbers are indicated on the spectra. The record was made at 1752 EST on 22 February 1965.

#### 4.2.9 Record No. 204

Figures 12a and 12b show the scattering functions calculated from Records 204, File 1, and 204, File 3. These files started at 11:50:05 and 11:53:25 EST respectively on 27 February 1965. There was

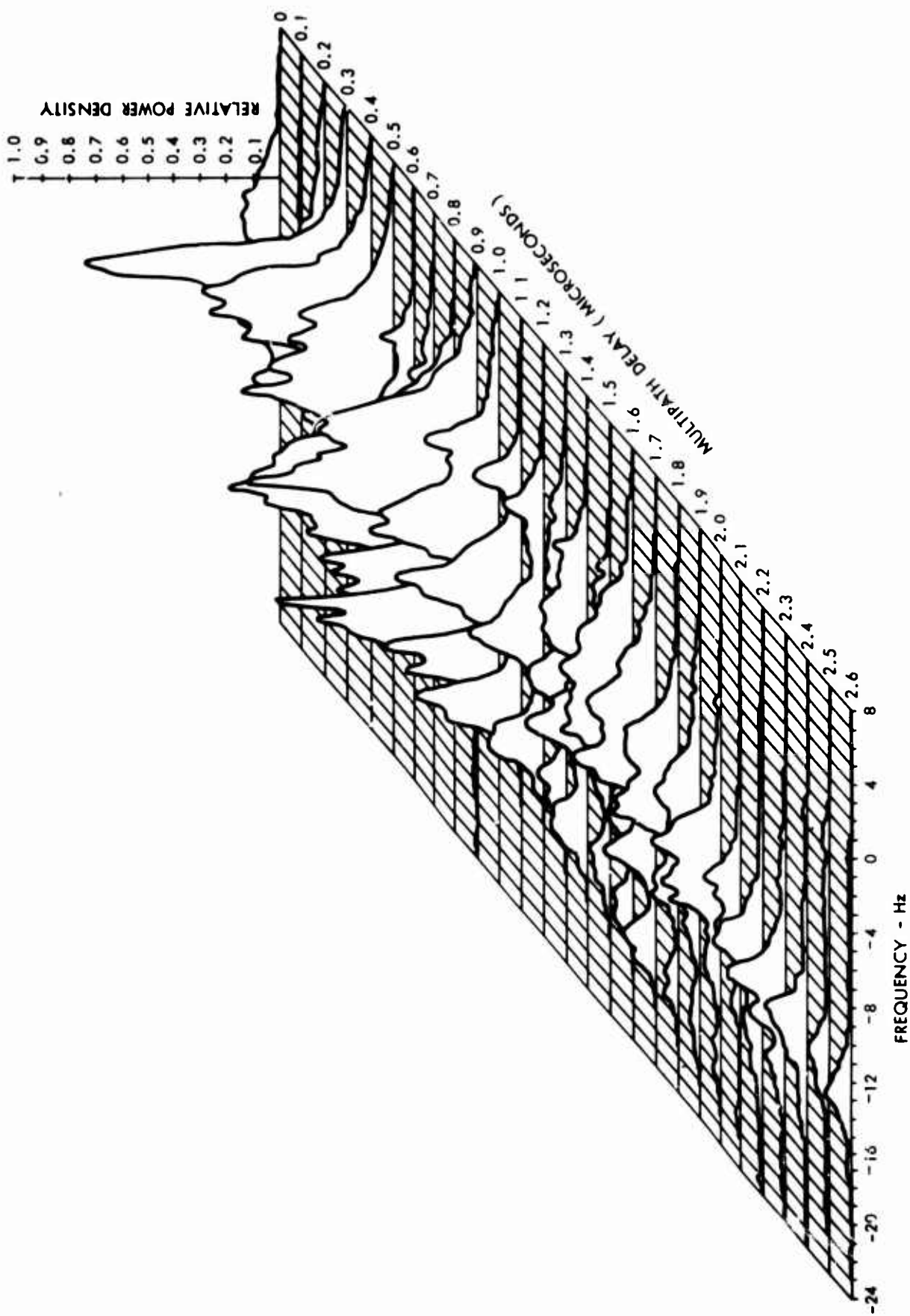


Figure 9. Scattering Function, Record No. 181

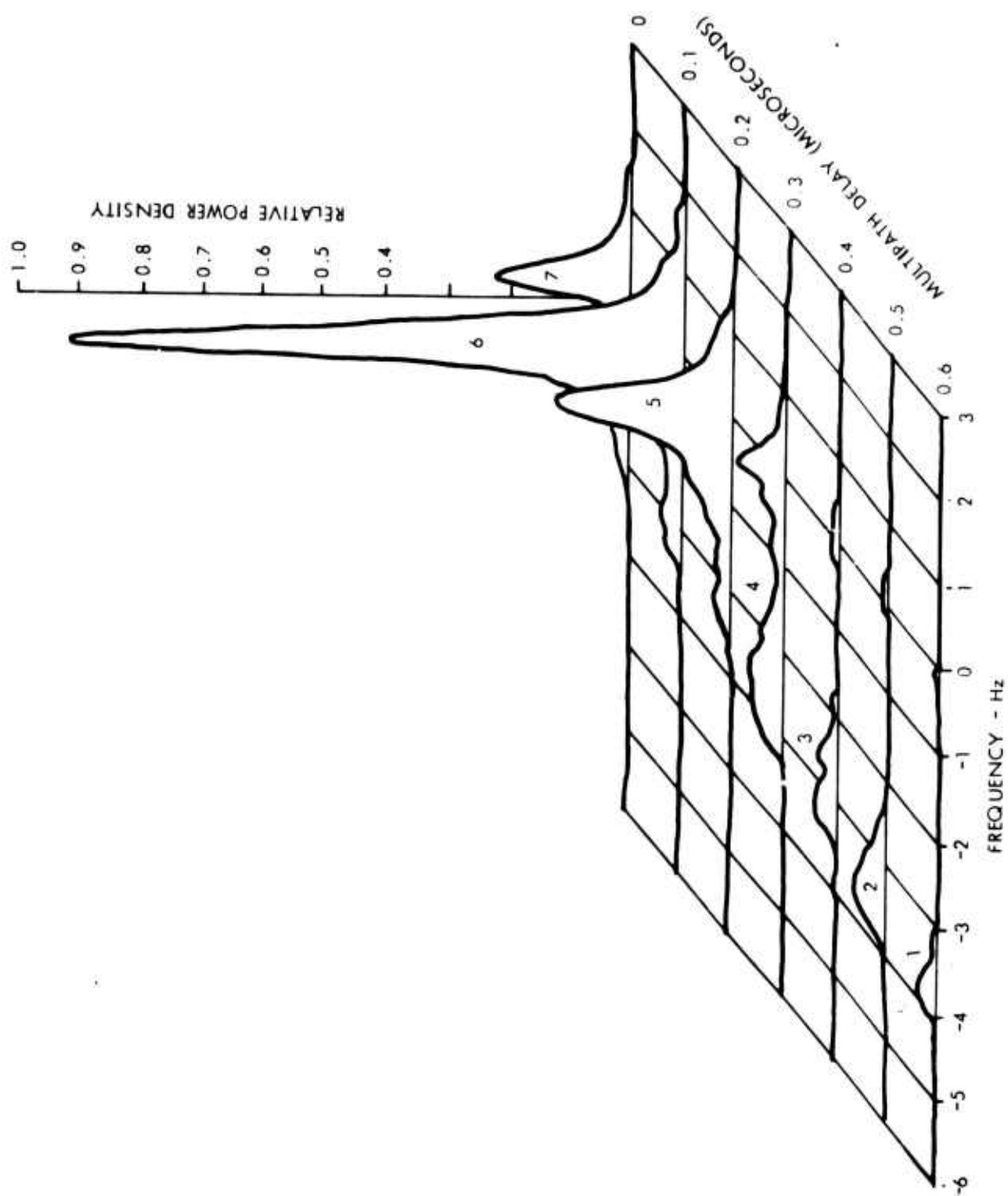


Figure 10. Scattering Function, Record No. 191

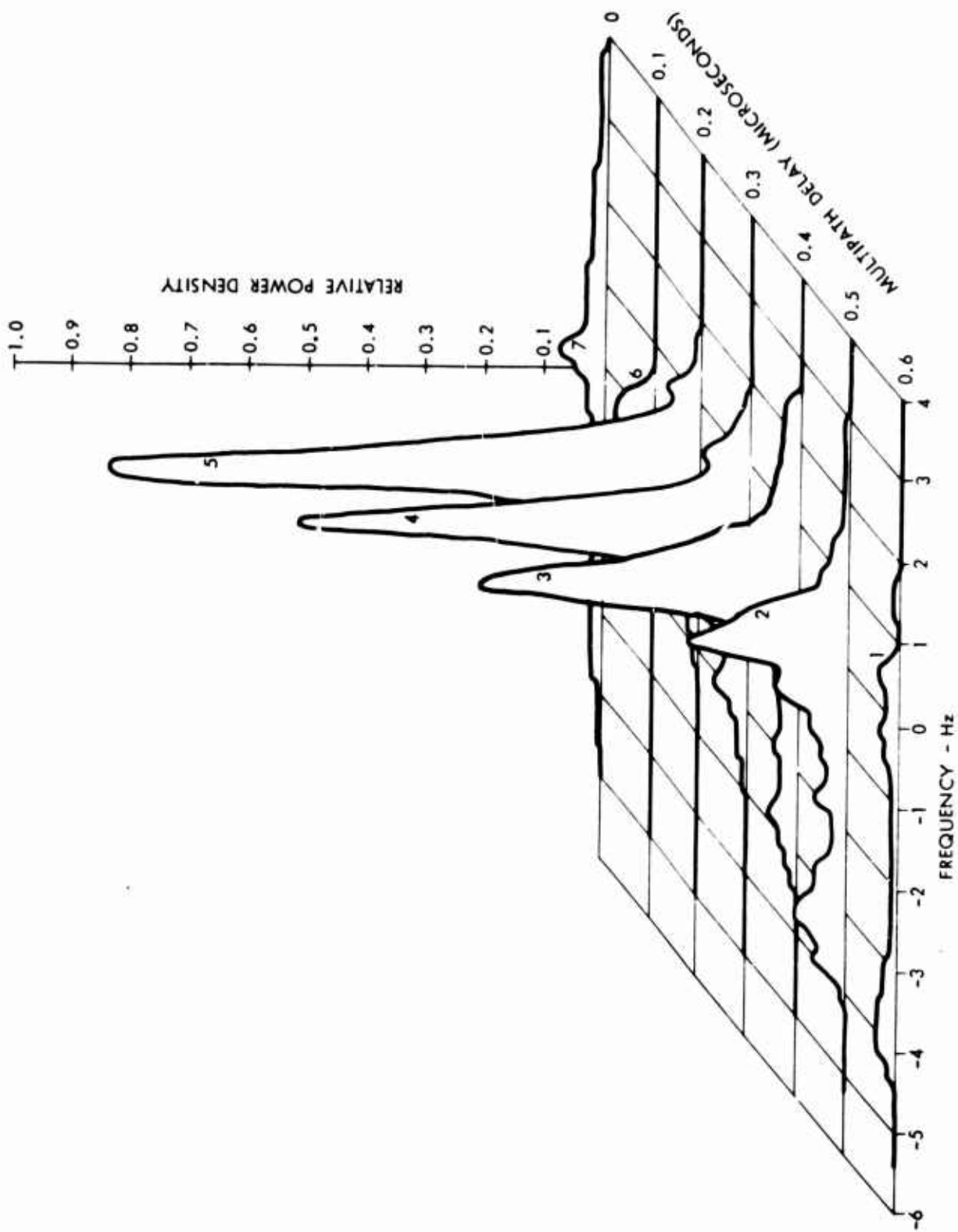


Figure 11. Scattering Function, Record No. 201

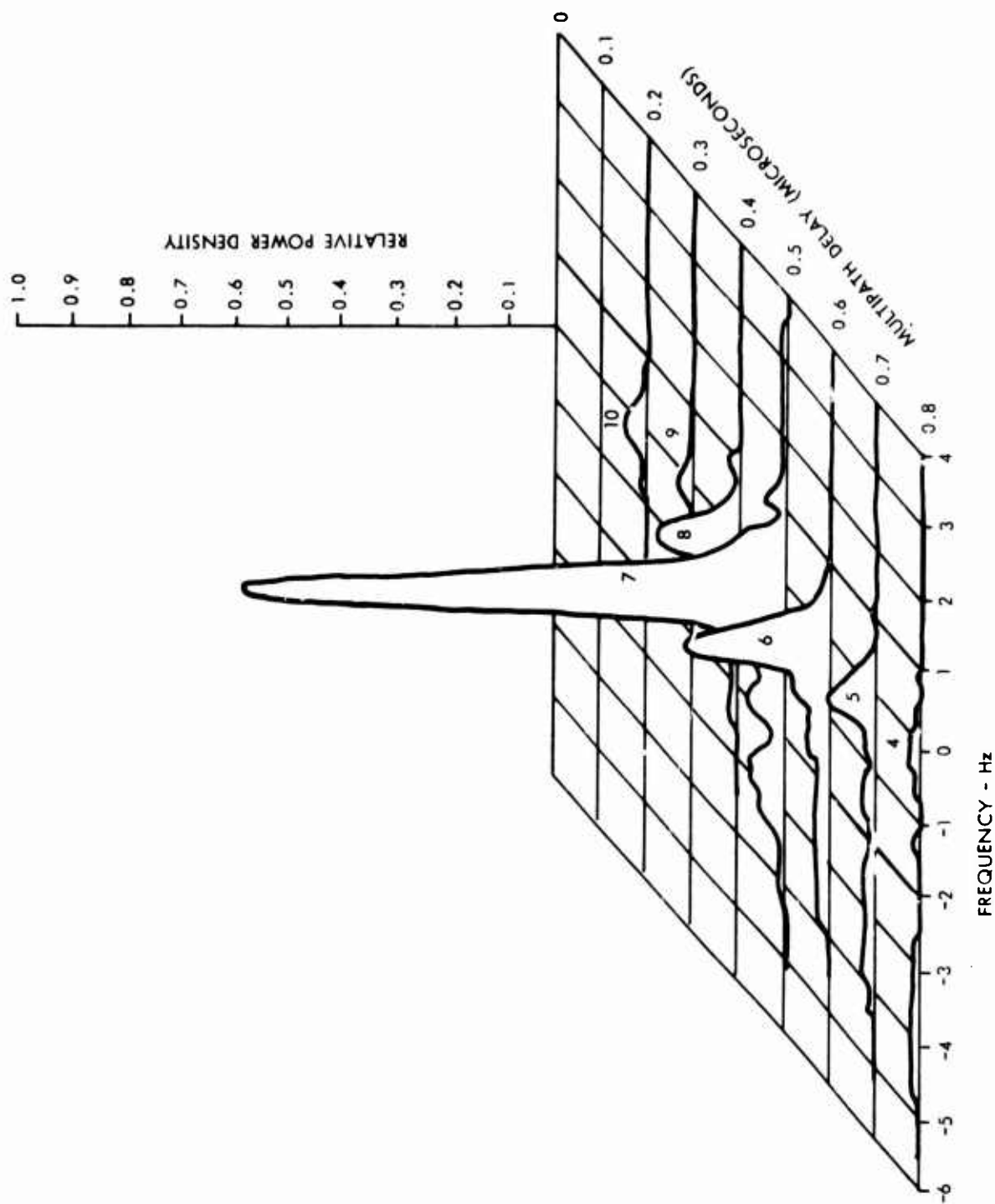


Figure 12a. Scattering Function, Record No. 204-1

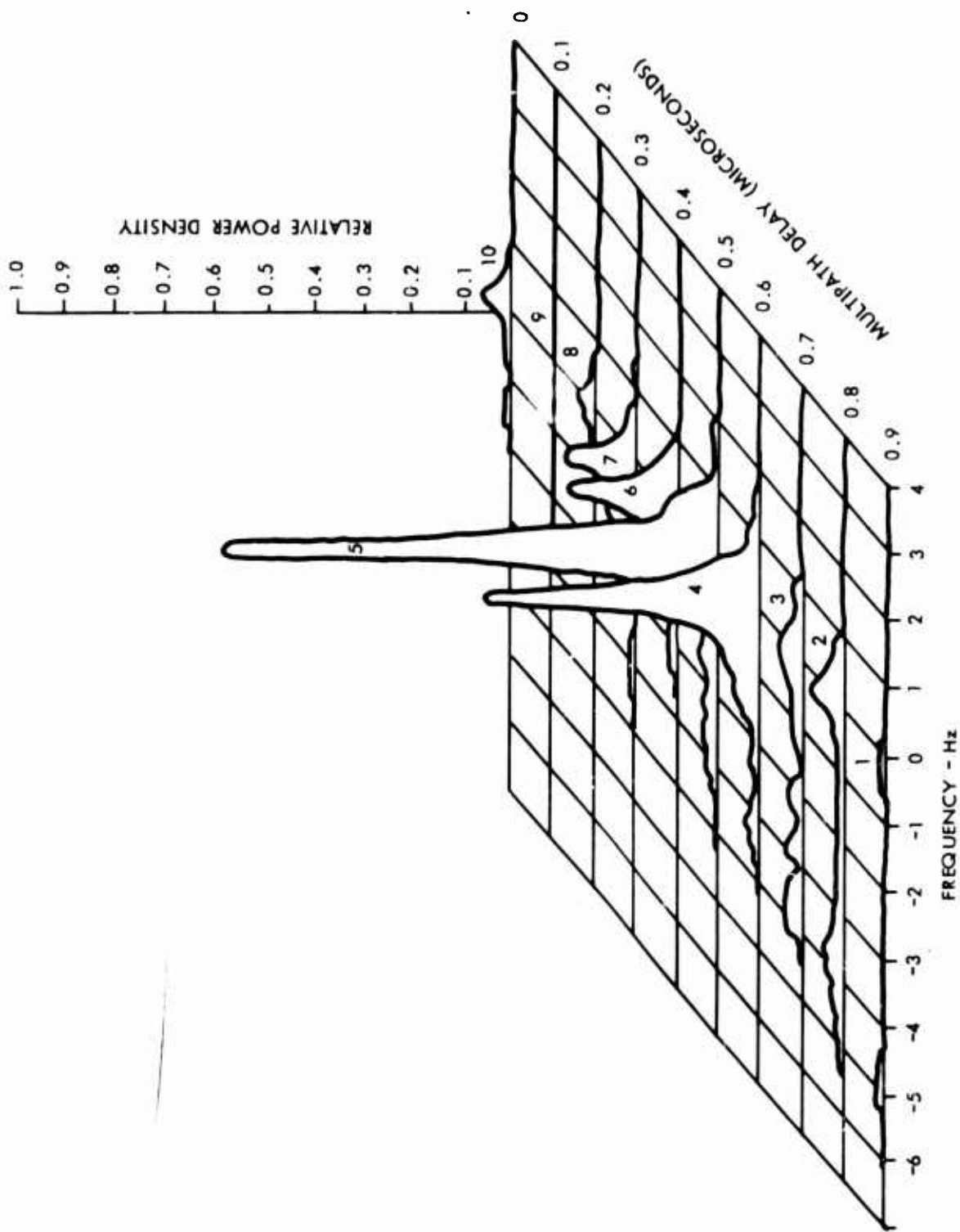


Figure 12b. Scattering Function, Record No. 204-3

no adjustment (retard or advance) of receiver timing between these files. (The tap numbers from the original data are indicated on the individual spectra.) The multipath delay scale and Doppler frequency scale have been drawn so as to give what we infer to be the approximately correct scattering function, following the technique used on previous multiple-record scattering functions. One conclusion to be drawn is that the medium is statistically stationary for the elapsed time involved in collecting the files of data.

The operator's log indicates that an aircraft flew through the portion of the common volume corresponding to tap number seven while File 1 was being recorded. The operator observed a strong signal in tap 7, shifted in Doppler frequency. Such signals were very apparent on the oscilloscope display of the quadrature components. Usually the beat frequency was observed to change rapidly (within a few seconds) and sometimes go through zero beat. Presumably the reason that the presence of the aircraft is not apparent in Figure 12a is that the aircraft did not stay at one Doppler and one delay position long enough to cause an indication of its presence when an averaging time of 100 seconds is used.

#### 4.2.10 Mean Frequency and Spectral Width for the Over-Land Data

Figures 13 and 14 present the mean frequency and RMS spectral width for all the over-land scattering functions discussed here. The outstanding feature of Figure 13 is that the mean frequency for any given run is relatively flat for the earliest few Rake taps and then decreases at a slope of roughly 4 Hz per  $\mu$ s.

We have examined the cross-path wind component for the period of time during which testing occurred. During the test series, the cross-path wind component, at all altitudes in the scattering volume,



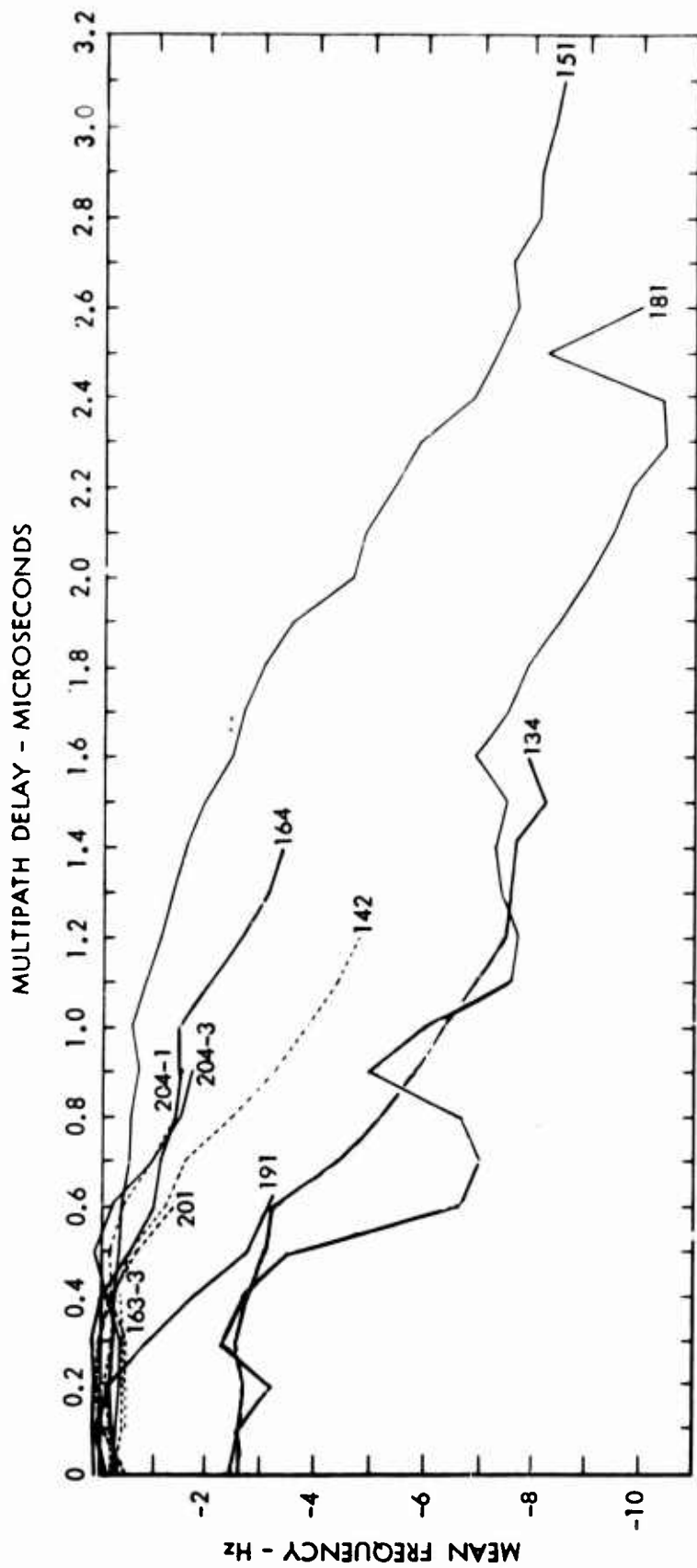


Figure 13. Mean Frequency vs. Multipath Delay (Over-Land Data)

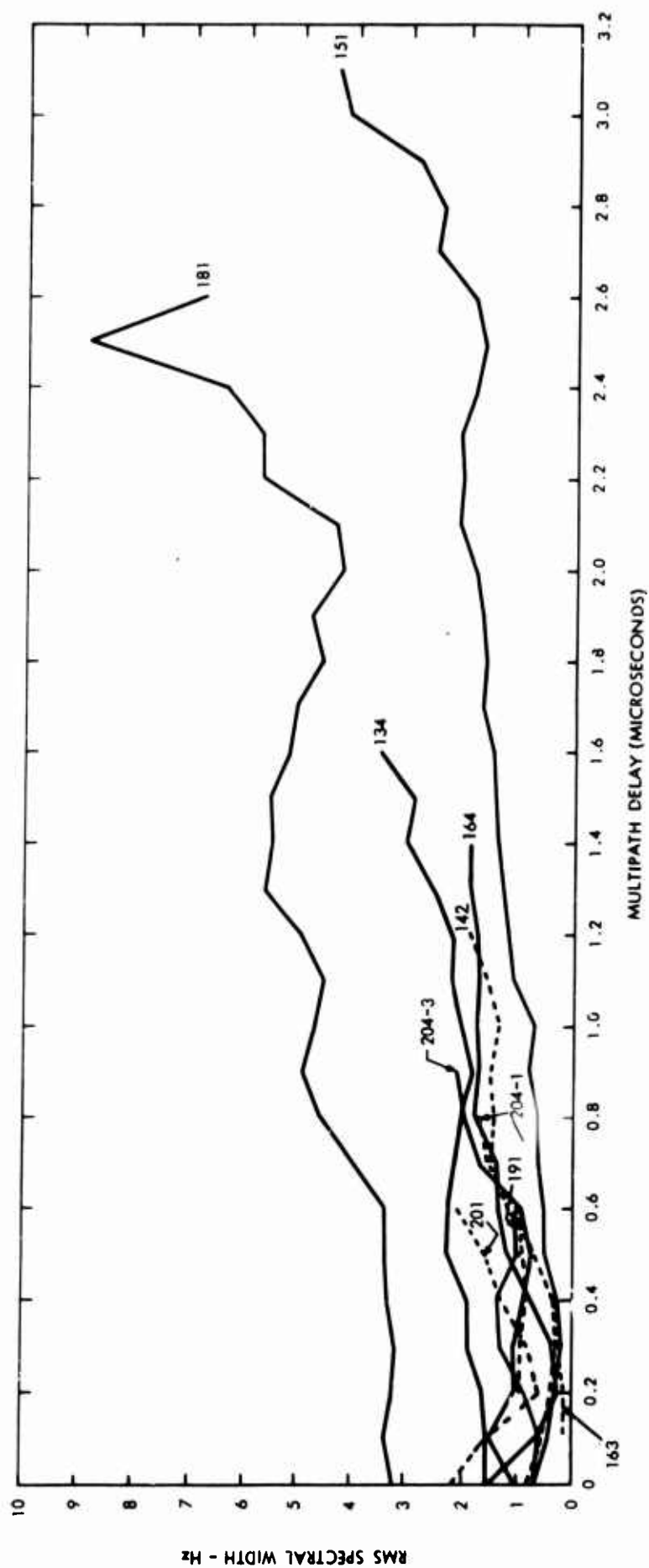


Figure 14. RMS Spectral Width vs. Multipath Delay (Over-Land Data)

is from west to east. It is our present conviction that the observed shift in mean frequency is accounted for by a combination of the cross path wind and a misalignment of the antennas. Some years ago Chisholm et al. (10) discussed the role of off-great-circle path contributions to fading. At that time they were dealing with envelope fading rates, although the geometrical picture presented was similar to that used today. It is interesting to note that the envelope fading rate increases slightly as the antennas are rotated away from the great circle path. A much larger effect is seen in the present studies because the absolute shift is detected as well as the Doppler spread. Interest in the correlation between winds and fading rate have continued to this day. For example, one of the authors published a correlation between the knee of the fading spectrum and the cross-path winds in 1959. (See Abraham and Bradshaw (11).) Recent work by Birkemeier et al. (9), that seems to deal directly with this problem of misalignment of the antennas and its effect on the coherent descriptions of signal, has come to our attention. Following his work we have drawn a cross-section of the scattering volume at midpath showing the lines of constant time delay and a hypothesized beam position. For the limited number of cases for which calculations were performed as of the present, we can approximately explain the spectral shapes observed if we hypothesize that the transmitting and receiving antennas were misaligned so that the active portion of the common volume was on the eastern side of the great circle path. This investigation is a continuing effort, and more work remains to be done.

A comparison of Figure 14 with Figure 13 shows that the spectral width is sometimes correlated with the mean frequency, especially at low multipath time delays, and is sometimes not correlated. Further work remains to be done in interpreting this result and in correlating the spectral width with the available wind data.

### 4.3 OVER-WATER TESTS

The test series conducted in November and December 1965 involved the 614 km over-water path previously discussed. A separate report<sup>7</sup> presents the detailed calculations from data collected on this path. Here, we will summarize some of the salient features of the results.

#### 4.3.1 Record No. 3022

Figure 15 presents the magnitude of the complex covariance function calculated from record number 3022. The covariance functions for all ten Rake taps have been superposed. All are normalized to the peak correlation, that for tap 7 in this case. Figure 16 presents the scattering function for this same record. This scattering function is typical of the narrow spectra obtained for the over-water data. The fading during this test series was characterized by the operator as slow fading, which is consistent with the narrow spectra calculated.

#### 4.3.2 Record No. 3703

Figure 17 gives the scattering function calculated from Record No. 3703. Of the set of over-water data for which calculations were performed, this scattering function has an atypically large Doppler spread.

#### 4.3.3 Mean Frequency and Spectral Width for the Over-Water Data

Figures 18 and 19 give the mean frequency and RMS spectral width for the complete set of over-water calculations performed to date. In contrast to the over-land results the mean frequencies are quite small and relatively flat as a function of multipath delay for the runs indicated.

It can be seen from Figure 19 that, except for Record 3703, all runs showed rather consistent slow fading (narrow spectra), as had been noted by the operator during the tests. The variations in the typical runs are not significant, although the low spectral width that seems to be general at  $0.6 \mu s$  (corresponding to tap 4 in all cases) cannot easily be explained. Certainly, it is a property of the equipment and not the medium.

Run 3703 does show a significant spectral broadening (faster fading) at long multipath delays.

No attempt has as yet been made to correlate these results with the weather data available.<sup>8</sup>



Figure 15. Relative Auto-Covariance vs. Time Shift, Record No. 3022

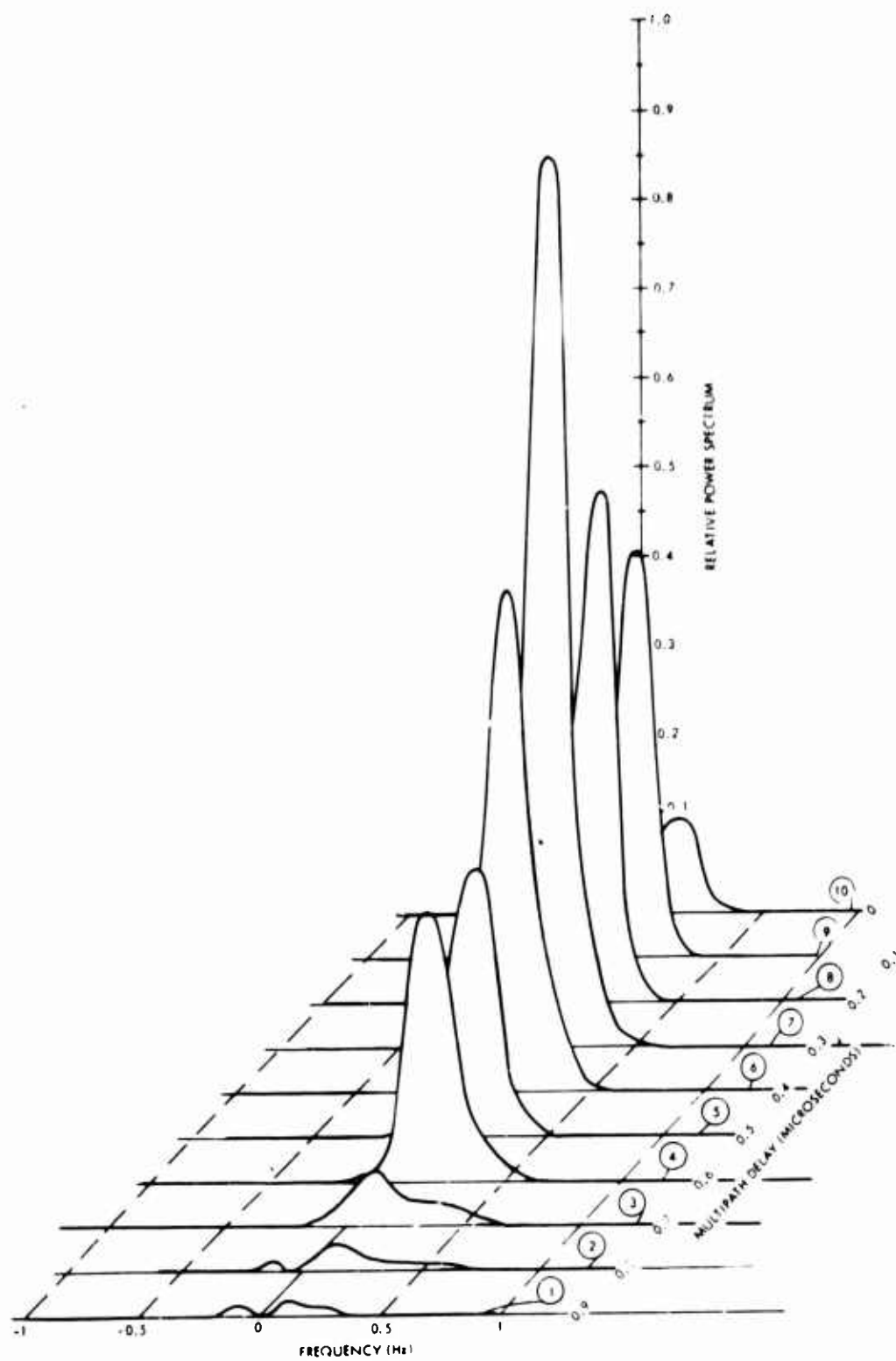


Figure 16. Scattering Function, Record No. 3022

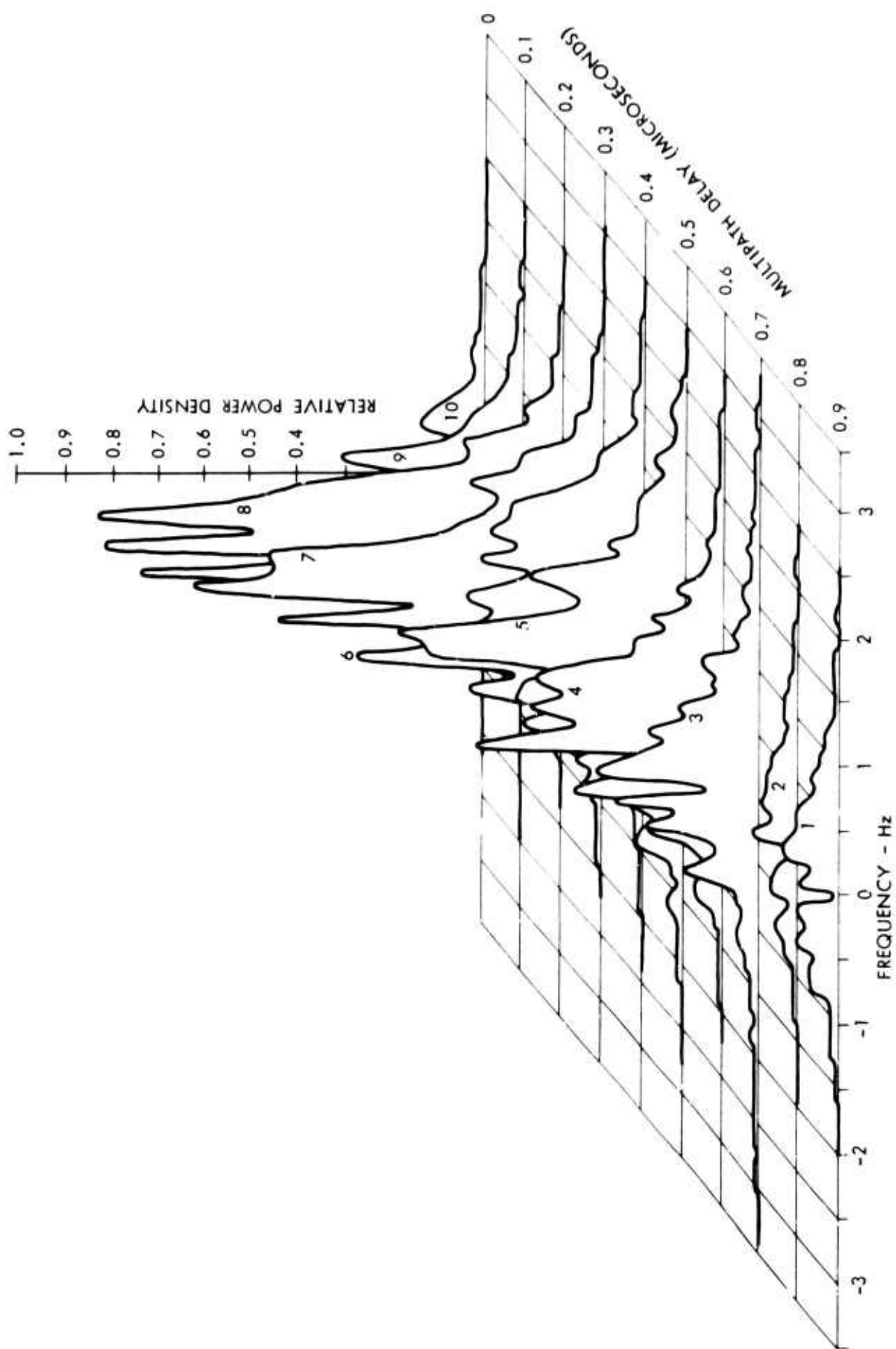


Figure 17. Scattering Function, Record No. 3703



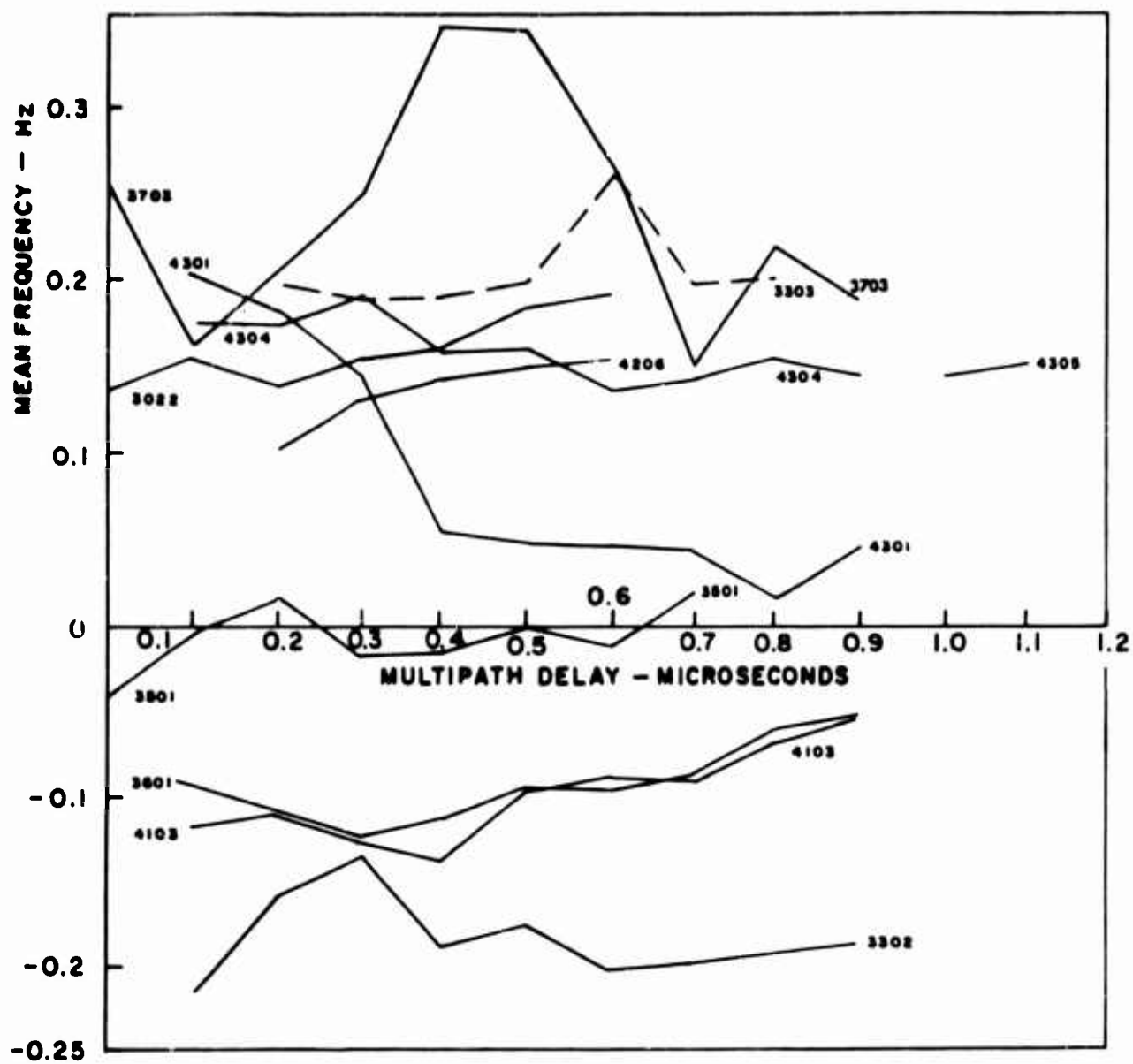


Figure 18. Mean Frequency as a Function of Multipath Time Delay (Over-Water Data)

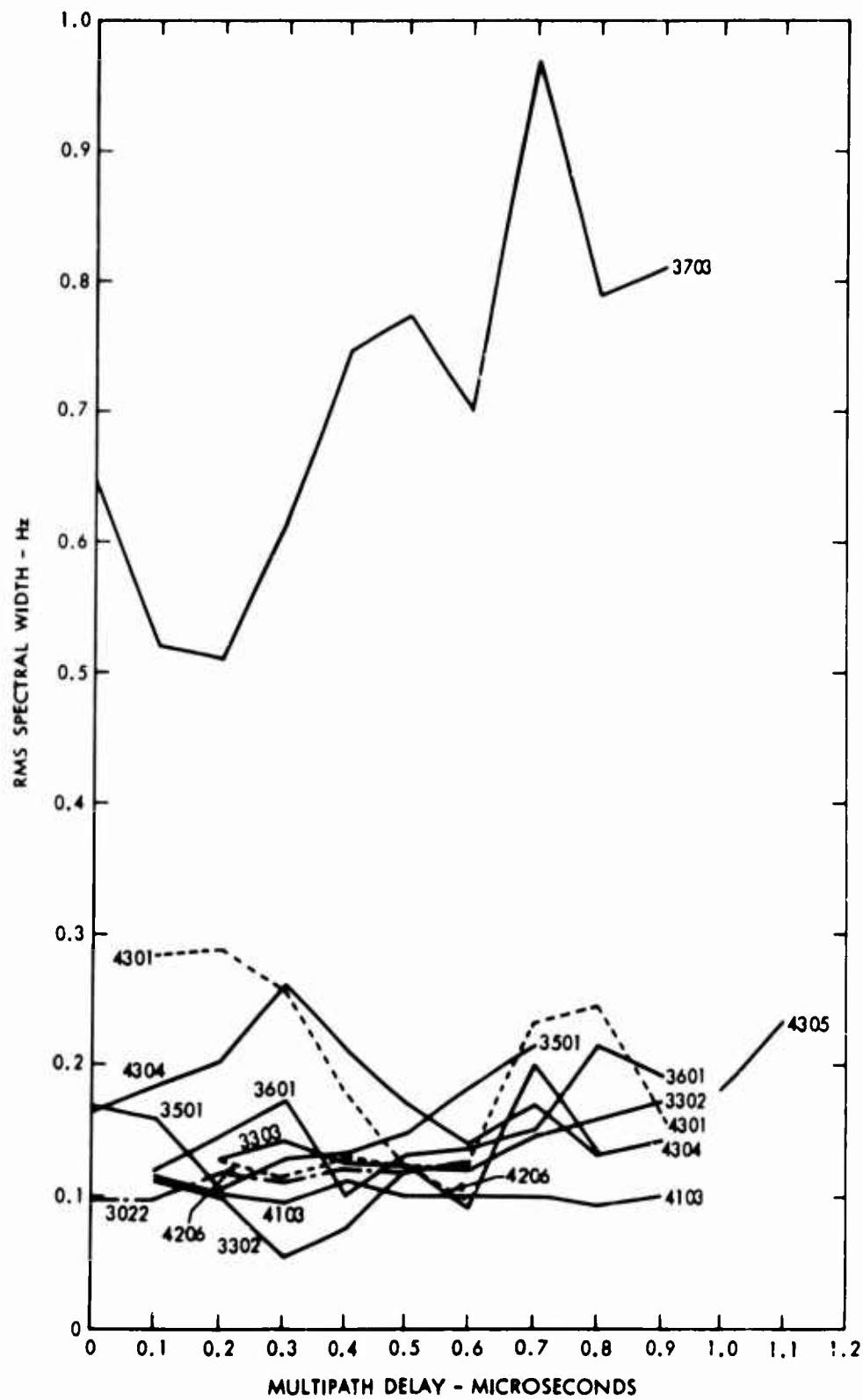


Figure 19. RMS Spectral Width as a Function of Multipath Time Delay (Over-Water Data)

## SECTION 5

### CONCLUSIONS

The scattering functions presented here and in Reference 7 are to the best of our knowledge the first such presentations obtained for tropospheric-scatter transmission paths. The unique features of the instrumentation that allowed us to obtain the scattering function were the path-delay resolution and the phase-coherent sampling of the output signals. Delay resolution was obtained by means of direct sequence modulation of the transmitted carrier coupled with a Rake receiver. By coherently sampling and recording the Rake "tap" outputs we were able to calculate, using a digital computer, the complex autocovariance function and its related spectrum. The advantage of coherent sampling is that Doppler shifts and asymmetric spectra can be observed.

Scattering functions are presented in this report for both an over-water and an over-land path, with chief emphasis on the latter. More data on the over-water path are available in Reference 7. The over-water data are characterized by very slow fading rates (typically a few tenths of a hertz) and by relatively narrow multipath spread (typically a microsecond or less). The limiting factor on multipath spread may at times have been the narrow antenna beams. At other times, however, the multipath spread was narrower than the estimated limitations implied by the antenna beamwidth would indicate.

The over-land data are characterized by faster fading rates (typically several hertz) and by wider multipath spread (typically 2 or 3 microseconds). The larger multipath spread is expected because of the wider antenna beam patterns. One of the most interesting discoveries found in the over-land data is the variation of mean Doppler frequency with path delay. Except for the first few taps corresponding

to shortest path delay, the mean frequency tends to decrease at a constant slope of roughly 4 Hz per  $\mu$ s. The spectral width, on the other hand, tends to remain more nearly constant as a function of multipath delay for any given record. We feel that the explanation for this behavior lies in the phenomenology discussed already in subsection 4.2.10. The fact that the spectral width remains more constant as a function of multipath delay than the absolute shift is extremely interesting. This spectral width is proportional to the envelope fading rate reported by Chisholm et al. (10). It has already been pointed out in the text that in their experiments the envelope fading rate had much less variation with rotation of the antennas. This would appear to agree with the fact that in our experiments the spectral width was more insensitive also to multipath delay. The geometrical picture is that, as the multipath delay increases, the apparent band of contributing turbulence is more and more completely displaced from the great circle plane. In effect, then, increasing multipath delay should roughly correspond to rotation of the antenna away from the great circle path direction.

Good oscillator accuracy and stability is of course necessary for the phase sensitive measurements we have made. The most severe requirements on oscillator stability comes, however, when we try to piece together scattering functions, which were recorded several minutes apart. This was necessary to obtain complete scattering functions when the total multipath spread exceeded 1  $\mu$ s, the maximum that could be accommodated in the Rake receiver at one time. As discussed earlier, a frequency error of one hertz (an error of 1 part in  $10^9$ ) would cause the multipath to drift approximately one tap within the duration of one record file, which was 100 seconds. When scattering functions from three records were pieced together, the delay between first and last record was approximately 12 minutes. To keep the drift in reference time less than 0.1  $\mu$ s (one Rake tap), the frequency accuracy

would have to be within 0.13 hertz (a frequency error less than 1.4 parts in  $10^{10}$ ).

By checking the file-to-file behavior of the scattering functions we have inferred a correction to the frequency axis and the multipath delay axis to present scattering functions that we feel are accurate to  $\pm$  a few tenths of a hertz in Doppler frequency. We feel that we have fitted together scattering functions consisting of multiple runs to approximately  $\pm 0.1 \mu\text{s}$  or one tap.

Several other aspects of the available data remain to be examined. First, further attempts to correlate the scattering functions with available weather data should be made. So far, only a tentative first look at some available weather data has been attempted in conjunction with the over-land data. Weather data<sup>8</sup> available covering the over-water tests should also be examined. Unfortunately the detailed atmospheric measurements given in Reference 8 were taken in December 1965, whereas the majority of our data collection was in November 1965.

In addition to presentations of scattering functions we have summarized in this report the reduced data in the form of mean frequency and RMS spectral width as a function of multipath delay. Another summary that should be useful in detecting important correlations is a table of three parameters characterizing the scattering functions: total power level, multipath spread, and total spectral width.

As interesting as the data collected so far on only two paths has proven to be, it in no way can be expected to characterize a fading channel model applicable to tropospheric scatter paths in use or contemplated for use throughout the world under many types of atmospheric conditions and path geometries. It would therefore be desirable to collect more such data--preferably under conditions where enough atmospheric measurements could also be made that perhaps the phenomenon of scatter communication could be better understood.

## SECTION 6

### REFERENCES

1. B. B. Barrow, L. Abraham, S. Stein and D. Bitzer, "Tropospheric-Scatter Propagation Tests Using A Rake Receiver," 1st Annual IEEE Communication Convention, Boulder, Colorado, June 7-9, 1965. Also available as Research Report 461, Applied Research Laboratory, Sylvania Electronic Systems, Waltham, Massachusetts; 16 April 1965.
2. B. B. Barrow, L. Abraham, S. Stein and D. Bitzer, "Preliminary Report on Tropospheric-Scatter Propagation Tests Using A Rake Receiver," Proc. IEEE, vol. 53, no. 6, pp. 649-651; June 1965.
3. B. B. Barrow, "Time-Delay Spread with Tropospheric Propagation Beyond the Horizon," Research Note 364, Applied Research Laboratory, Sylvania Electronic Systems, Waltham, Massachusetts; October 1962.
4. R. B. Blackman and J. W. Tukey, "The Measurement of Power Spectra," Dover Publications, New York; 1959.
5. A. D. Wheelon, "Radio-Wave Scattering by Tropospheric Irregularities," Journal Res. NBS, Part D. Radio Propagation, vol. 63D, no. 2, pp. 205-233; September-October 1959.
6. D. R. Bitzer, D. A. Chesler, R. Ivers and S. Stein, "A Rake System for Tropospheric-Scatter," IEEE Trans. on Comm. Tech., vol. COM-14, no. 4, pp. 499-506; August 1966.
7. L. G. Abraham, B. B. Barrow, W. M. Cowan, and R. M. Gallant, "Tropospheric Scatter Multipath Tests in the Caribbean," Sylvania Electronic Systems, Applied Research Laboratory, Waltham, Massachusetts; June 1966.
8. O. A. Tagliaferri, "Support to DCS Tropospheric Scatter Tests," Tech. Report No. RADC-TR-66-609, Rome Air Development Center; October 1966. AD# 640 942

9. W. P. Birkemeier et al., "Observation of Wind Produced Doppler Shifts in Troposcatter," Univ. of Wisconsin, Depts. of Electrical Engineering and Meteorology; March 1967.
10. J. H. Chisholm et al., "Investigations of Angular Scattering and Multipath Properties of Tropospheric Propagation of Short Radio Waves Beyond the Horizon," Proc. IRE, vol. 43, pp. 1317-1335; October 1955.
11. L. G. Abraham, Jr., and J. A. Bradshaw, "Tropospheric Scatter Propagation Study," prepared by General Electric Co. under Contract No. AF19(604)-1723, Final Report No. AFCRC-TR-59-353 (AD 232 924); October 1959.



UNCLASSIFIED

Security Classification

## DOCUMENT CONTROL DATA - R &amp; D

(Security classification of title, body of abstract and indexing annotation must be entered when the overall report is classified)

1. ORIGINATING ACTIVITY (Corporate author) Sylvania Electronic Systems, Applied Research Lab, A Division of Sylvania Electric Products, Inc. 40 Sylvan Road, Waltham, Massachusetts 02154		2a. REPORT SECURITY CLASSIFICATION Unclassified	
		2b. GROUP N/A	
3. REPORT TITLE  Anti-Jam Techniques for Troposcatter Communications, Volume III - Tropospheric Scatter Multipath Tests			
4. DESCRIPTIVE NOTES (Type of report and inclusive dates) Final Report			
5. AUTHOR(S) (First name, middle initial, last name) Leonard G. Abraham, Jr.                      Bruce B. Barrow William M. Cowan                              Robert M. Gallant			
6. REPORT DATE September 1967		7a. TOTAL NO. OF PAGES 68	7b. NO. OF REFS 11
8a. CONTRACT OR GRANT NO. AF30(602)-3992		9a. ORIGINATOR'S REPORT NUMBER(S)	
b. PROJECT NO. 4519 Task No. 451902			
d.		9b. OTHER REPORT NO(S) (Any other numbers that may be assigned this report) RADC-TR-67-130, Volume III	
10. DISTRIBUTION STATEMENT This document is subject to special export controls and each transmittal to foreign governments, foreign nationals or representatives thereto may be made only with prior approval of RADC (EMLI), GAFB, N.Y. 13440.			
11. SUPPLEMENTARY NOTES RADC PROJECT ENGINEER WALTER R. RICHARD EMCRS/AC 315 330-2807		12. SPONSORING MILITARY ACTIVITY Rome Air Development Center (EMCRS) Griffiss Air Force Base, New York 13440	
13. ABSTRACT  The final report for this effort is prepared in three volumes. Volume III contains the results of troposcatter multipath measurements. Scattering functions are presented for data collected on other programs using a Rake receiver on two paths, one along the eastern seaboard, and the other in the Caribbean.  Volume I of the final report contains the analytical results and performance predictions for the tropo A-J systems. Volume II contains the various A-J system descriptions.			

DD FORM 1 NOV 65 1473

UNCLASSIFIED

Security Classification



UNCLASSIFIED

Security Classification

14	KEY WORDS	LINK A		LINK B		LINK C	
		ROLE	WT	ROLE	WT	ROLE	WT
	Troposcatter Communications Anti-Jam Techniques Frequency Hopping Error Correction Coding Spread Spectrum Direct Sequence Modulation						

UNCLASSIFIED

Security Classification